

## Development and evaluation of novel InhA inhibitors inspired by thiadiazole and tetrahydropyran series of inhibitors

MARTINA HRAST RAMBAHER<sup>1</sup>   
NINA GRADIŠEK<sup>1</sup>   
ROK FRLAN<sup>1</sup>   
IZIDOR SOSIČ<sup>1</sup>   
ALJOŠA BOLJE<sup>1</sup>   
JAKOB KLJUN<sup>2</sup>   
MARTIN JUHÁŠ<sup>1,3,4</sup>   
STANISLAV GOBEC<sup>1</sup>   
STANE PAJK<sup>1,\*</sup> 

<sup>1</sup> University of Ljubljana, Faculty of Pharmacy, 1000 Ljubljana, Slovenia

<sup>2</sup> University of Ljubljana, Faculty of Chemistry and Chemical Technology, 1000 Ljubljana, Slovenia

<sup>3</sup> Charles University, Faculty of Pharmacy in Hradec Králové, 500 05 Hradec Králové Czech Republic

<sup>4</sup> University of Hradec Králové, Faculty of Science, 500 03 Hradec Králové, Czech Republic

### ABSTRACT

Tuberculosis (TB), caused by *Mycobacterium tuberculosis*, remains a leading global health challenge, exacerbated by the emergence of multidrug-resistant (MDR) and extensively drug-resistant (XDR) strains. One promising therapeutic target is the enzyme enoyl-acyl carrier protein reductase (InhA), which plays a vital role in the biosynthesis of mycolic acids, essential components of the bacterial cell wall. Direct inhibition of InhA offers a potential strategy for overcoming resistance mechanisms, particularly in cases where the activation of conventional drugs like isoniazid is compromised. This study investigates two novel series of InhA inhibitors based on thiadiazole and tetrahydropyran lead compounds, originally identified through high-throughput screening by GSK. Analogues were synthesised using the copper-catalysed azide-alkyne cycloaddition (CuAAC) click reaction, and their inhibitory activity was tested against InhA. Among the tested compounds, only one exhibited modest inhibitory activity, with an  $IC_{50}$  of 11  $\mu\text{mol L}^{-1}$ , while others were inactive. Interestingly, during the synthetic efforts, a novel reaction was discovered between aryl methyl ketones and ethynylmagnesium bromide, yielding 1,3-diols, as confirmed by X-ray diffraction analysis. These findings underscore the challenges of optimising InhA inhibitors and highlight the potential of synthetic innovations in exploring new synthetic pathways.

**Keywords:** tuberculosis, InhA, direct inhibitors, click reaction, 1,3-diol synthesis

Accepted May 21, 2025  
Published online May 21, 2025

### INTRODUCTION

Tuberculosis (TB), caused by *Mycobacterium tuberculosis* (*M. tuberculosis*), remains one of the world's leading infectious diseases, with millions of new cases and deaths annually (1). This pathogen is distinguished by its robust cell wall, rich in mycolic acids, which contributes to its resistance to many drugs and environmental stresses (2). The increasing prevalence of multidrug-resistant (MDR) and extensively drug-resistant (XDR) TB underscores the urgent need for novel therapeutic targets and treatments (3).

\* Correspondence; e-mail: stane.pajk@ffa.uni-lj.si

One promising target in TB drug development is the enzyme enoyl-acyl carrier protein reductase (InhA), a key component in the fatty acid synthesis pathway in *M. tuberculosis*. InhA is directly involved in synthesising mycolic acids, which are essential for maintaining the bacterial cell wall's integrity and thus its survival (4). InhA has gained attention due to its role in resistance to the frontline anti-TB drug isoniazid (INH). INH functions as a prodrug and must undergo enzymatic activation by KatG, a bifunctional catalase-peroxidase. Under KatG-mediated catalysis, INH is oxidised to form a reactive isonicotinoyl radical, which subsequently reacts with NADH to generate a nicotinoyl-NAD adduct that binds to and inhibits InhA. Mutations in the KatG gene, responsible for activating INH, often render the drug ineffective, a major issue in TB treatment (5). Direct inhibition of InhA, bypassing KatG activation, offers a potential strategy for overcoming INH resistance (6).

Various chemical classes have emerged as direct InhA inhibitors, binding directly to the enzyme to block its activity without requiring KatG activation. Early studies identified triclosan analogues (Fig. 1) as effective InhA inhibitors, with structural optimisations yielding compounds with enhanced potency (7, 8). Ibrahim and colleagues synthesised diphenyl ether derivatives linked to oxadiazoles (9), achieving significant antitubercular activity, while other researchers explored macrocyclic and di-triclosan derivatives to improve selectivity and potency (10, 11). High-throughput screening also identified novel inhibitors, such as Genz-10850 (GEQ) (Fig. 1), leading to the development of derivatives with nanomolar-range InhA inhibitory activity (12, 13).

Three novel classes of direct InhA inhibitors have recently shown promising *in vivo* efficacy in murine TB models, making them potential candidates for TB drug development. One such compound, NITD-916 (Fig. 1), a 4-hydroxy-2-pyridone, was identified through high-throughput screening and demonstrated efficacy in mouse models of *M. tuberculosis*, *M. abscessus*, and *M. fortuitum* infections (14, 15). In 2018, boron-containing compounds were introduced as another novel InhA inhibitor class, with AN12855 emerging as a lead compound (Fig. 1). AN12855 exhibited strong bactericidal activity against drug-resistant *M. tuberculosis* strains by targeting InhA's substrate-binding site and demonstrated favourable pharmacokinetics, achieving dose-dependent efficacy in both acute and chronic murine TB models comparable to INH (16).

In 2013, a thiadiazole series capable of inhibiting InhA independently of KatG activation was identified. Structural studies revealed unique binding interactions within InhA, establishing a novel mode of inhibition and demonstrating potent antimycobacterial activity (17, 18). In 2015, a thorough structure-activity relationship (SAR) study expanded on this series, optimising the thiadiazole scaffold to enhance potency and drug-like properties. The best compound exhibited nanomolar-range InhA inhibition, submicromolar MICs, and favourable pharmacokinetics, marking significant progress in developing direct InhA inhibitors (19). Recently, further development of this inhibitor class yielded GSK693 and GSK138 (Fig. 1), which were tested in murine TB models and demonstrated efficacy in combination with first-line and novel TB regimens (20). GSK138, in particular, showed enhanced pharmacokinetics and bactericidal activity, supporting the potential of direct InhA inhibitors to combat drug-resistant TB and enhance existing treatment options. The same high-throughput screening campaign at GlaxoSmithKline (GSK) that led to the discovery of GSK693 and GSK138 also identified a tetrahydropyran-based direct InhA inhibitor (Fig. 1, **compd. 1**) with a similar binding mode but a completely different scaffold (21).

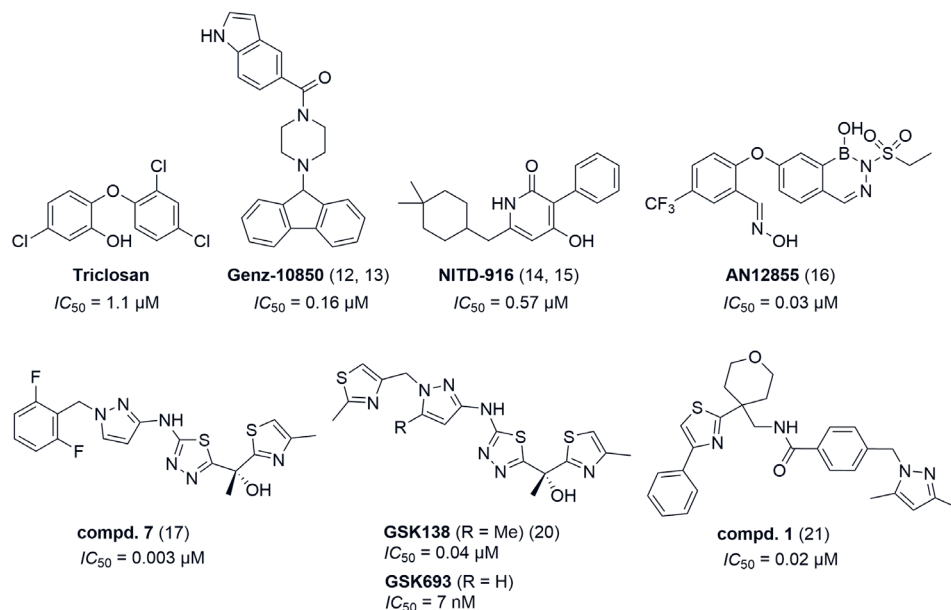


Fig. 1. Chemical structures of representative direct InhA inhibitors with their  $IC_{50}$  values (12–17, 20, 21).

In this study, we designed, synthesised, and evaluated two series of compounds for their inhibitory activity against the InhA enzyme. These series were based on thiaziazole (Fig. 1, GSK138, GSK693 and **compd. 7**) and tetrahydropyran (Fig. 1, **compd. 1**) lead compounds initially identified by GSK through high-throughput screening. The CuAAC click reaction was employed to rapidly and efficiently synthesise new analogues. While compounds showed poor inhibitory activity against InhA, the synthesis process led to the discovery of an intriguing reaction between aryl methyl ketones and the Grignard reagent ethynylmagnesium bromide, resulting in the formation of 1,3-diols. The structure of two of these products was confirmed by X-ray diffraction analysis, providing valuable insights for future investigations.

## EXPERIMENTAL

### Materials and methods

All chemicals were purchased from Sigma-Aldrich, Apollo Scientific, TCI, BLDpharm, and Acros and were used as received without further purification. Analytical thin-layer chromatography (TLC) was performed on Merck silica gel plates (60 F<sub>254</sub>, 0.25 mm) and visualised under ultraviolet light. NMR spectra (<sup>1</sup>H and <sup>13</sup>C) were recorded on a Bruker AVANCE III 400 MHz NMR spectrometer using CDCl<sub>3</sub>, DMSO-*d*<sub>6</sub>, or methanol-*d*<sub>4</sub> as solvents. Chemical shifts were referenced to tetramethylsilane (TMS) or residual solvent

peaks. Mass spectrometry (MS) data were acquired using a Thermo Scientific Q Exactive Plus mass spectrometer.

*General procedure A.* – 2.7 mol L<sup>-1</sup> *n*-butyllithium (*n*-BuLi) in hexane (3.75 mL, 1.5 equiv, 7.5 mmol) was added dropwise to a solution of ethynyltrimethylsilane (1.41 mL, 1.0 equiv, 10.0 mmol) in anhydrous tetrahydrofuran (THF, 5 mL) at -78 °C under an inert atmosphere. The mixture was stirred for 15 minutes before the dropwise addition of the appropriate ketone (1.0 equiv, 5.0 mmol) dissolved in anhydrous THF (5 mL). The reaction mixture was allowed to gradually warm to room temperature and stirred for 15 hours. The reaction was quenched by adding a saturated solution of ammonium chloride (2 mL), followed by the addition of 1 mol L<sup>-1</sup> tetrabutylammonium fluoride (TBAF) in THF (25 mL). The mixture was stirred for an additional 30 minutes. The solvent was removed under reduced pressure, and the residue was dissolved in ethyl acetate (EtOAc, 60 mL). The organic layer was washed sequentially with water (2 × 30 mL) and brine (30 mL), then dried over anhydrous sodium sulphate. The solvent was evaporated under reduced pressure to yield the crude product.

*General procedure B.* – Tris(triphenylphosphine)copper(I) bromide (0.05 equiv) was added to a mixture of the appropriate alkyne (1.0 equiv) and azide (1.0 equiv). The reaction mixture was stirred under neat conditions at 40 °C for 15 hours. If the azide and alkyne did not form a homogeneous mixture, a few drops of dichloromethane (DCM) were added to create a uniform solution. The DCM was then allowed to evaporate, and the reaction was continued under neat conditions.

*General procedure C.* – The appropriate alkyne (1.0 equiv) and azide (1.0 equiv) were dissolved in a mixture of EtOAc and methanol (MeOH) (4:1, 5 mL per 1 mmol of azide). Copper(I) bromide (0.05 equiv) and triethylamine (0.1 equiv) were added, and the reaction mixture was stirred at 40 °C for 15 hours. After completion, the reaction mixture was diluted with EtOAc and washed sequentially with 5 % trisodium citrate solution and brine. The organic layer was dried over anhydrous sodium sulphate, and the solvent was removed under reduced pressure to afford the crude product.

*General procedure D.* – To a solution of aryl methyl ketone (1.0 equiv, 3 mmol) in tetrahydrofuran (THF, 2 mL) at 0 °C, 0.5 mol L<sup>-1</sup> ethynylmagnesium bromide in THF (12 mL, 2.0 equiv, 6 mmol) was added dropwise. The reaction mixture was stirred for 15 hours, after which a saturated solution of ammonium chloride (1 mL) was added, and the THF was removed under reduced pressure. The residue was suspended in EtOAc (50 mL), transferred to a separatory funnel, and washed sequentially with water (2 × 20 mL) and brine (30 mL). The organic phase was dried over anhydrous sodium sulphate, and the solvent was evaporated under reduced pressure.

The list of the prepared compounds 1–8 is given in Table I and their spectral data in Table II.

*Ethyl 1-(2,6-difluorobenzyl)-1H-pyrazole-3-carboxylate (1).* – Sodium hydride (NaH, 1.76 g, 60 % in paraffin, 1.3 equiv, 42 mmol) was added to a solution of ethyl 1H-pyrazole-3-carboxylate (5.22 g, 1.1 equiv, 37.2 mmol) in anhydrous tetrahydrofuran (THF) cooled in an ice bath. The reaction mixture was stirred at 0 °C for 30 minutes, after which 2-(bromomethyl)-1,3-difluorobenzene (7.00 g, 1.0 equiv, 33.8 mmol) was added. The reac-

tion mixture was then allowed to warm to room temperature and stirred for 15 hours. The reaction was quenched by adding 2 mL of a saturated solution of ammonium chloride, and the solvents were removed under reduced pressure. The resulting residue was suspended in EtOAc (150 mL). The organic phase was washed sequentially with water (40 mL), a saturated solution of sodium bicarbonate (40 mL), 1 mol L<sup>-1</sup> hydrochloric acid (40 mL), and brine (40 mL), then dried over anhydrous sodium sulphate. The solvent was evaporated under reduced pressure, and the residue was washed with hexane (3 × 30 mL) to afford the desired product (92 %) as a white solid.

*(1-(2,6-Difluorobenzyl)-1H-pyrazol-3-yl)methanol (2)*. – A solution of iodine (2.38 g, 1.0 equiv, 9.4 mmol) in tetrahydrofuran (THF, 25 mL) was added dropwise to a suspension of ethyl 1-(2,6-difluorobenzyl)-1H-pyrazole-3-carboxylate (2.5 g, 1.0 equiv, 9.4 mmol) and sodium borohydride (852 mg, 2.4 equiv, 22.5 mmol) in THF (30 mL) cooled in an ice bath. Once hydrogen evolution ceased, the reaction mixture was refluxed for 15 hours. The reaction mixture was then cooled in an ice bath and quenched by the dropwise addition of MeOH until the solution became completely clear. The solvents were evaporated under reduced pressure, and the residue was treated with 5 % sulfuric acid (30 mL). The resulting suspension was stirred for 1 hour. DCM (150 mL) was added, and the mixture was transferred to a separatory funnel. The organic phase was washed sequentially with a saturated solution of sodium bicarbonate (40 mL) and brine (40 mL), then dried over anhydrous sodium sulphate. The solvent was removed under reduced pressure, and the crude product was purified by flash column chromatography on silica gel (eluent: EtOAc/hexane, gradient from 1:2 to 3:2) to yield the desired product (79 %) as a white solid.

*3-(Azidomethyl)-1-(2,6-difluorobenzyl)-1H-pyrazole (3)*. – Methanesulfonyl chloride (600 mg, 1.5 equiv, 5.2 mmol) was added dropwise to a solution of (1-(2,6-difluorobenzyl)-1H-pyrazol-3-yl)methanol (782 mg, 1.0 equiv, 3.5 mmol) and *N,N*-diisopropylethylamine (DIPEA, 1.21 mL, 2.0 equiv, 7.0 mmol) in DCM (30 mL) cooled in an ice bath. The reaction progress was monitored by TLC, which after 30 minutes indicated complete consumption of the starting alcohol. The reaction mixture was transferred to a separatory funnel, and an additional 30 mL of DCM was added. The organic phase was washed sequentially with a saturated solution of sodium bicarbonate (40 mL), 1 mol L<sup>-1</sup> hydrochloric acid (40 mL), and brine (40 mL), then dried over anhydrous sodium sulphate. The solvent was evaporated under reduced pressure, and the residue was dissolved in dimethylformamide (25 mL). Sodium azide (NaN<sub>3</sub>, 680 mg, 3.0 equiv, 10.5 mmol) was added to the solution, and the reaction mixture was stirred at 65 °C for 15 hours. The mixture was then diluted with EtOAc (100 mL), transferred to a separatory funnel, and washed with water (5 × 40 mL) and brine (40 mL). The organic layer was dried over anhydrous sodium sulphate, and the solvent was removed under reduced pressure. The crude product was purified by flash column chromatography on silica gel (eluent: EtOAc/hexane, gradient from 1:6 to 1:2) to afford the desired product (67 %) as a colourless liquid.

*2-(4-Methylthiazol-2-yl)but-3-yn-2-ol (4a)*. – (23) 2.7 mol L<sup>-1</sup> *n*-BuLi in hexane (13.2 mL, 1.2 equiv, 35.6 mmol) was added dropwise to a solution of 4-methylthiazole (2.75 mL, 1.0 equiv, 30.2 mmol) in anhydrous tetrahydrofuran (THF, 100 mL) at -78 °C under an inert atmosphere. The reaction mixture was stirred at -78 °C for 30 minutes, followed by the dropwise addition of 1-(trimethylsilyl)propan-2-one (5.0 mL, 1.0 equiv, 30.2 mmol). The mixture was allowed to gradually warm to room temperature and stirred for an addi-

tional 15 hours. The reaction was quenched by the addition of a saturated solution of ammonium chloride (10 mL), followed by 1 mol L<sup>-1</sup> TBAF in THF (25 mL). The resulting mixture was stirred for 30 minutes. The solvent was removed under reduced pressure, and the residue was dissolved in EtOAc (100 mL). The organic layer was washed sequentially with water (2 × 70 mL) and brine (70 mL), then dried over anhydrous sodium sulphate. After solvent removal under reduced pressure, the crude product was purified by flash column chromatography on silica gel (eluent: EtOAc/hexane, gradient from 1:4 to 1:2), affording the desired product (55 %) as a white solid.

2-(*Pyridin-2-yl*)but-3-yn-2-ol (**4b**). – (24) The compound was prepared according to the General procedure A. The crude product was purified by flash column chromatography on silica gel (eluent: EtOAc/hexane, gradient from 1:2 to 1:1), affording the desired product in 44 % yield.

2-(*Pyridin-3-yl*)but-3-yn-2-ol (**4c**). – (25) The compound was prepared according to the General procedure A. The crude product was purified by flash column chromatography on silica gel (eluent: EtOAc/hexane, gradient from 1:2 to 1:1), affording the desired product in 32 % yield.

2-(*Pyridin-4-yl*)but-3-yn-2-ol (**4d**). – (26) The compound was prepared according to the General procedure A. The crude product was purified by flash column chromatography on silica gel (eluent: EtOAc/hexane, 1:1), affording the desired product in 31 % yield.

2-(3-*Fluoropyridin-2-yl*)but-3-yn-2-ol (**4e**). – (27) The compound was prepared according to the General procedure A. The crude product was purified by flash column chromatography on silica gel (eluent: EtOAc/hexane, 1:5), affording the desired product in 69 % yield.

2-(*Pyrazin-2-yl*)but-3-yn-2-ol (**4f**). – (28) The compound was prepared according to the general procedure A. The crude product was purified by flash column chromatography on silica gel (eluent: EtOAc/hexane, gradient from 1:4 to 1:2), affording the desired product in 29 % yield.

2-(*Pyrimidin-2-yl*)but-3-yn-2-ol (**4g**). – (29) The compound was prepared according to the General procedure A. The crude product was purified by flash column chromatography on silica gel (eluent: EtOAc/hexane, 1:1), affording the desired product in 33 % yield.

2-(2-*Methoxyphenyl*)but-3-yn-2-ol (**4h**). – (25) The compound was prepared according to the General procedure A. The crude product was purified by flash column chromatography on silica gel (eluent: EtOAc/hexane, 1:8), affording the desired product in 37 % yield.

2-(4-*Methoxyphenyl*)but-3-yn-2-ol (**4i**). – (30) The compound was prepared according to the General procedure A. The crude product was purified by flash column chromatography on silica gel (eluent: EtOAc/hexane, gradient from 1:6 to 1:4), affording the desired product in 34 % yield.

2-(*m-Tolyl*)but-3-yn-2-ol (**4j**). – (31) The compound was prepared according to the General procedure A. The crude product was purified by flash column chromatography on silica gel (eluent: EtOAc/hexane, gradient from 1:6 to 1:4), affording the desired product in 7 % yield.

2-(Benzo[d][1,3]dioxol-5-yl)but-3-yn-2-ol (**4k**). – (32) The compound was prepared according to the General procedure A. The crude product was purified by flash column chromatography on silica gel (eluent: EtOAc/hexane, gradient from 1:6 to 1:4), affording the desired product in 29 % yield.

2-(4-(Dimethylamino)phenyl)but-3-yn-2-ol (**4l**). – (33) The compound was prepared according to the General procedure A. The crude product was purified by flash column chromatography on silica gel (eluent: EtOAc/hexane, 1:4), affording the desired product in 26 % yield.

2-(5-Bromothiophen-2-yl)but-3-yn-2-ol (**4m**). – The compound was prepared according to the General procedure A. The crude product was purified by flash column chromatography on silica gel (eluent: EtOAc/hexane, 1:6), affording the desired product in 35 % yield.

2-(Thiophen-2-yl)but-3-yn-2-ol (**4n**). – (34) The compound was prepared according to the General procedure A. The crude product was purified by flash column chromatography on silica gel (eluent: EtOAc/hexane, 1:6), affording the desired product in 59 % yield.

2-(4-Nitrophenyl)but-3-yn-2-ol (**4o**). – (35) The compound was prepared according to the General procedure A. The crude product was purified by flash column chromatography on silica gel (eluent: EtOAc/hexane, 1:6), affording the desired product in 42 % yield.

2-(2,6-Difluorophenyl)but-3-yn-2-ol (**4p**). – (36) The compound was prepared according to the General procedure A. The crude product was purified by flash column chromatography on silica gel (eluent: EtOAc/hexane, 1:8), affording the desired product in 69 % yield.

1-(1-((1-(2,6-Difluorobenzyl)-1H-pyrazol-3-yl)methyl)-1H-1,2,3-triazol-4-yl)-1-(4-methylthiazol-2-yl)ethan-1-ol (**5a**). – The compound was prepared according to the General procedure B. The crude product was purified by flash column chromatography on silica gel (eluent: EtOAc/hexane, 2:1), affording the desired product in 88 % yield.

1-(1-((1-(2,6-Difluorobenzyl)-1H-pyrazol-3-yl)methyl)-1H-1,2,3-triazol-4-yl)-1-(pyridin-2-yl)ethan-1-ol (**5b**). – The compound was prepared according to the General procedure C. The crude product was purified by flash column chromatography on silica gel (eluent: EtOAc/hexane, 4:1), affording the desired product in 36 % yield.

1-(1-((1-(2,6-Difluorobenzyl)-1H-pyrazol-3-yl)methyl)-1H-1,2,3-triazol-4-yl)-1-(pyridin-3-yl)ethan-1-ol (**5c**). – The compound was prepared according to the General procedure B. The crude product was purified by flash column chromatography on silica gel (eluent: EtOAc/hexane, gradient from 2:1 to 1:0), affording the desired product in 84 % yield.

1-(1-((1-(2,6-Difluorobenzyl)-1H-pyrazol-3-yl)methyl)-1H-1,2,3-triazol-4-yl)-1-(pyridin-4-yl)ethan-1-ol (**5d**). – The compound was prepared according to the General procedure C. The crude product was purified by flash column chromatography on silica gel (eluent: EtOAc/hexane, 2:1), affording the desired product in 39 % yield.

1-(1-((1-(2,6-Difluorobenzyl)-1H-pyrazol-3-yl)methyl)-1H-1,2,3-triazol-4-yl)-1-(3-fluoropyridin-2-yl)ethan-1-ol (**5e**). – The compound was prepared according to the General procedure B. The crude product was purified by flash column chromatography on silica gel (eluent: EtOAc/hexane, gradient from 1:1 to 2:1), affording the desired product in 97 % yield.

1-(1-((1-(2,6-Difluorobenzyl)-1H-pyrazol-3-yl)methyl)-1H-1,2,3-triazol-4-yl)-1-(pyrazin-2-yl)ethan-1-ol (**5f**). – The compound was prepared according to the General procedure B. The crude product was purified by flash column chromatography on silica gel (eluent: EtOAc/hexane, 2:1), affording the desired product in 68 % yield.

1-(1-((1-(2,6-Difluorobenzyl)-1H-pyrazol-3-yl)methyl)-1H-1,2,3-triazol-4-yl)-1-(pyrimidin-2-yl)ethan-1-ol (**5g**). – The compound was prepared according to the General procedure B. The crude product was purified by flash column chromatography on silica gel (eluent: EtOAc/hexane, 2:1), affording the desired product in 62 % yield.

1-(1-((1-(2,6-Difluorobenzyl)-1H-pyrazol-3-yl)methyl)-1H-1,2,3-triazol-4-yl)-1-(2-methoxyphenyl)ethan-1-ol (**5h**). – The compound was prepared according to the General procedure B. The crude product was purified by flash column chromatography on silica gel (eluent: EtOAc/hexane, gradient from 1:1 to 2:1), affording the desired product in 97 % yield.

1-(1-((1-(2,6-Difluorobenzyl)-1H-pyrazol-3-yl)methyl)-1H-1,2,3-triazol-4-yl)-1-(4-methoxyphenyl)ethan-1-ol (**5i**). – The compound was prepared according to the General procedure B. The crude product was purified by flash column chromatography on silica gel (eluent: EtOAc/hexane, gradient from 2:1 to 3:2), affording the desired product in 67 % yield.

1-(1-((1-(2,6-Difluorobenzyl)-1H-pyrazol-3-yl)methyl)-1H-1,2,3-triazol-4-yl)-1-(*m*-tolyl)ethan-1-ol (**5j**). – The compound was prepared according to the General procedure B. The crude product was purified by flash column chromatography on silica gel (eluent: EtOAc/hexane, gradient from 1:1 to 2:1), affording the desired product in 58 % yield.

1-(Benzo[d][1,3]dioxol-5-yl)-1-(1-((1-(2,6-difluorobenzyl)-1H-pyrazol-3-yl)methyl)-1H-1,2,3-triazol-4-yl)ethan-1-ol (**5k**). – The compound was prepared according to the General procedure B. The crude product was purified by flash column chromatography on silica gel (eluent: EtOAc/hexane, 1:1), affording the desired product in 51 % yield.

1-(1-((1-(2,6-Difluorobenzyl)-1H-pyrazol-3-yl)methyl)-1H-1,2,3-triazol-4-yl)-1-(4-(dimethylamino)phenyl)ethan-1-ol (**5l**). – The compound was prepared according to the General procedure B. The crude product was purified by flash column chromatography on silica gel (eluent: EtOAc/hexane, 2:1), affording the desired product in 77 % yield.

1-(5-Bromothiophen-2-yl)-1-(1-((1-(2,6-difluorobenzyl)-1H-pyrazol-3-yl)methyl)-1H-1,2,3-triazol-4-yl)ethan-1-ol (**5m**). – The compound was prepared according to the General procedure B. The crude product was purified by flash column chromatography on silica gel (eluent: EtOAc/hexane, 1:1), affording the desired product in 73 % yield.

1-(1-((1-(2,6-Difluorobenzyl)-1H-pyrazol-3-yl)methyl)-1H-1,2,3-triazol-4-yl)-1-(thiophen-2-yl)ethan-1-ol (**5n**). – The compound was prepared according to the General procedure B. The crude product was purified by flash column chromatography on silica gel (eluent: EtOAc/hexane, 1:1), affording the desired product in 85 % yield.

1-(1-((1-(2,6-Difluorobenzyl)-1H-pyrazol-3-yl)methyl)-1H-1,2,3-triazol-4-yl)-1-(4-nitrophenyl)ethan-1-ol (**5o**). – The compound was prepared according to the General procedure B. The crude product was purified by flash column chromatography on silica gel (eluent: EtOAc/hexane, 1:1), affording the desired product in 70 % yield.

1-(1-((1-(2,6-Difluorobenzyl)-1H-pyrazol-3-yl)methyl)-1H-1,2,3-triazol-4-yl)-1-(2,6-difluorophenyl)ethan-1-ol (**5p**). – The compound was prepared according to the General procedure B. The crude product was purified by flash column chromatography on silica gel (eluent: EtOAc/hexane, 1:1), affording the desired product in 72 % yield.

2,4-Bis(4-methylthiazol-2-yl)hex-5-yne-2,4-diol (mixture of diastereomers) (**6a**). – The compound was prepared according to General procedure D. The crude product was purified by flash column chromatography on silica gel (eluent: EtOAc/hexane, gradient from 1:3 to 1:1), affording the desired product in 11 % yield.

2,4-Di(pyridin-2-yl)hex-5-yne-2,4-diol (**6b**). – The compound was prepared according to General procedure D. Crystals of the compound formed in the oily residue after the initial workup of the reaction mixture and were subsequently isolated, affording the desired product in 26 % yield.

2,4-bis(3-Fluoropyridin-2-yl)hex-5-yne-2,4-diol (**6c**). – The compound was prepared according to General procedure D. Crystals of the compound formed in the oily residue after the initial workup of the reaction mixture and were subsequently isolated, affording the desired product in 31 % yield.

2,4-bis(4-Nitrophenyl)hex-5-yne-2,4-diol (**6d**). – The compound was prepared according to General procedure D. The crude product was purified by flash column chromatography on silica gel (eluent: EtOAc/hexane, gradient from 1:3 to 1:1), affording the desired product in 13 % yield.

2,4-bis(2,6-Difluorophenyl)hex-5-yne-2,4-diol (**6e**). – Crystals of the compound formed in the oily residue after the initial workup of the reaction mixture and were subsequently isolated, affording the desired product in 17 % yield.

2,4-Bis(3,5-bis(trifluoromethyl)phenyl)hex-5-yne-2,4-diol (**6f**). – The compound was prepared according to General procedure D. The crude product was purified by flash column chromatography on silica gel (eluent: EtOAc/hexane, gradient from 1:6 to 1:1), affording the desired product in 78 % yield.

4-(Azidomethyl)-N-((4-(4-phenylthiazol-2-yl)tetrahydro-2H-pyran-4-yl)methyl)benzamide (**7**). – 4-(Azidomethyl)benzoic acid (740 mg, 1.0 equiv, 4.2 mmol) was dissolved in DCM (20 mL), followed by the addition of DMF (50  $\mu$ L) and dropwise addition of oxalyl chloride (540  $\mu$ L, 1.5 equiv, 6.3 mmol). The reaction mixture was stirred on an ice bath for 10 minutes and then refluxed at 40 °C for an additional 20 minutes. After the reaction was complete, the solvent was evaporated under reduced pressure. The resulting 4-(azidomethyl)benzoyl chloride was used in the subsequent reaction without purification.

In a separate flask, (4-(4-phenylthiazol-2-yl)tetrahydro-2H-pyran-4-yl)methanamine (1.15 g, 1.0 equiv, 4.2 mmol) was dissolved in DCM (50 mL), to which 4-(azidomethyl)benzoyl chloride and triethylamine (1.16 mL, 2.0 equiv, 8.3 mmol) were added. The reaction mixture was stirred in DCM at 0 °C for 15 minutes and then at room temperature for 2 hours. The reaction mixture was washed in a separatory funnel sequentially with 5 % Na<sub>2</sub>CO<sub>3</sub> solution (50 mL), 1 mol L<sup>-1</sup> HCl (30 mL), and a saturated NaCl solution (30 mL). The organic phase was dried over anhydrous sodium sulphate. The solvent was evaporated under reduced pres-

sure. The crude product was purified by flash column chromatography on silica gel (eluent: EtOAc/hexane, from 1:2 to 2/1), affording the desired product in 48 % yield.

4-((1H-1,2,3-Triazol-1-yl)methyl)-N-((4-(4-phenylthiazol-2-yl)tetrahydro-2H-pyran-4-yl)methyl)benzamide (**8a**). – The compound was prepared according to General procedure B with minor modifications. The reaction was initiated with azide **7** (134 mg, 1.0 equiv, 0.31 mmol) and trimethylsilylacetylene (132  $\mu$ L, 3.0 equiv, 0.93 mmol) as the alkyne reagent. Upon completion of the CuAAC reaction, the mixture was dissolved in tetrahydrofuran (5 mL), followed by the addition of 1 mol L<sup>-1</sup> TBAF in THF (2 mL). The resulting mixture was stirred at room temperature for 4 hours. Subsequently, the solvents were removed under reduced pressure, and the crude product was purified by flash column chromatography on silica gel (eluent: EtOAc/hexane, gradient from 1:1 to 1:0), affording the desired product in 33 % yield.

4-(((4-(Dimethylamino)methyl)-1H-1,2,3-triazol-1-yl)methyl)-N-((4-(4-phenylthiazol-2-yl)tetrahydro-2H-pyran-4-yl)methyl)benzamide (**8b**). – The compound was prepared according to General procedure C, with minor modifications, specifically the use of 2 equivalents of 3-dimethylamino-1-propyne. The crude product was purified by flash column chromatography on silica gel (eluent: DCM/MeOH, gradient from 20:1 to 10:1), affording the desired product in 61 % yield.

1-(4-(((4-(4-Phenylthiazol-2-yl)tetrahydro-2H-pyran-4-yl)methyl)carbamoyl)benzyl)-1H-1,2,3-triazole-4-carboxamide (**8c**). – The compound was prepared according to General procedure C, with minor modifications, specifically the use of 3 equivalents of propiolamide. The crude product was purified by flash column chromatography on silica gel (eluent: DCM/MeOH, gradient from 20:1 to 10:1), affording the desired product in 70 % yield.

Ethyl 1-(4-(((4-(4-phenylthiazol-2-yl)tetrahydro-2H-pyran-4-yl)methyl)carbamoyl)benzyl)-1H-1,2,3-triazole-4-carboxylate (**8d**). – The compound was prepared according to General procedure C, with minor modifications, specifically the use of 3 equivalents of ethyl propiolate. The crude product was purified by flash column chromatography on silica gel (eluent: EtOAc/hexane, gradient from 2:1 to 1:0), affording the desired product in 38 % yield.

1-(4-(((4-(4-Phenylthiazol-2-yl)tetrahydro-2H-pyran-4-yl)methyl)carbamoyl)benzyl)-1H-1,2,3-triazole-4-carboxylic acid (**8e**). – Ester **8d** (55 mg, 1.0 equiv, 0.10 mmol) was dissolved in ethanol (5 mL) and to the resulting mixture 2 mol L<sup>-1</sup> NaOH (1.03 mL, 20.0 equiv, 2.1 mmol) was added dropwise. After the completion of the reaction, the ethanol was evaporated under reduced pressure, and the pH of the residue was adjusted to 2 with 1 mol L<sup>-1</sup> HCl. The mixture was transferred to a separatory funnel and extracted with EtOAc (2  $\times$  20 mL), the combined organic phases were washed with a saturated solution of NaCl and dried over Na<sub>2</sub>SO<sub>4</sub>. Solvent was evaporated under reduced pressure to yield the desired product in 74 % yield.

Ester **8d** (55 mg, 1.0 equiv, 0.10 mmol) was dissolved in ethanol (5 mL), and 2 mol L<sup>-1</sup> NaOH (1.03 mL, 20.0 equiv, 2.1 mmol) was added dropwise to the resulting mixture. Upon completion of the reaction, ethanol was evaporated under reduced pressure, and the pH of the residue was adjusted to 2 using 1 mol L<sup>-1</sup> HCl. The mixture was transferred to a separatory funnel and extracted with EtOAc (2  $\times$  20 mL). The combined organic phases were washed with a saturated NaCl solution and dried over anhydrous sodium sulphate

(Na<sub>2</sub>SO<sub>4</sub>). The solvent was removed under reduced pressure, affording the desired product in 74 % yield.

4-((4-Cyclopropyl-1H-1,2,3-triazol-1-yl)methyl)-N-((4-(4-phenylthiazol-2-yl)tetrahydro-2H-pyran-4-yl)methyl)benzamide (**8f**). – The compound was prepared according to General procedure C, with minor modifications, specifically the use of 3 equivalents of cyclopropylacetylene. The crude product was purified by flash column chromatography on silica gel (eluent: EtOAc/hexane, gradient from 3:1 to 1:0), affording the desired product in 36 % yield.

4-((4-(3-Methoxyphenyl)-1H-1,2,3-triazol-1-yl)methyl)-N-((4-(4-phenylthiazol-2-yl)tetrahydro-2H-pyran-4-yl)methyl)benzamide (**8g**). – The compound was prepared according to General procedure C, with minor modifications, specifically the use of 3 equivalents of 3-ethynylanisole. The crude product was purified by flash column chromatography on silica gel (eluent: EtOAc/hexane, gradient from 1:1 to 3:1), affording the desired product in 83 % yield.

4-((4-Phenyl-1H-1,2,3-triazol-1-yl)methyl)-N-((4-(4-phenylthiazol-2-yl)tetrahydro-2H-pyran-4-yl)methyl)benzamide (**8h**). – The compound was prepared according to General procedure C, with minor modifications, specifically the use of 3 equivalents of phenylacetylene. The crude product was purified by flash column chromatography on silica gel (eluent: EtOAc/hexane, gradient from 1:1 to 3:1), affording the desired product in 81 % yield.

N-((4-(4-phenylthiazol-2-yl)tetrahydro-2H-pyran-4-yl)methyl)-4-((4-(pyridin-2-yl)-1H-1,2,3-triazol-1-yl)methyl)benzamide (**8i**). – The compound was prepared according to General procedure C, with minor modifications, specifically the use of 3 equivalents of 2-ethynylpyridine. The crude product was purified by flash column chromatography on silica gel (eluent: DCM/MeOH, gradient from 20:1 to 10:1), affording the desired product in 49 % yield.

Table I. The list of the prepared compounds 1–8

Compd.	Chemical name	Molecular formula
<b>1</b>	Ethyl 1-(2,6-difluorobenzyl)-1H-pyrazole-3-carboxylate	C <sub>13</sub> H <sub>12</sub> F <sub>2</sub> N <sub>2</sub> O <sub>2</sub>
<b>2</b>	(1-(2,6-Difluorobenzyl)-1H-pyrazol-3-yl)methanol	C <sub>11</sub> H <sub>10</sub> F <sub>2</sub> N <sub>2</sub> O <sub>2</sub>
<b>3</b>	3-(Azidomethyl)-1-(2,6-difluorobenzyl)-1H-pyrazole	C <sub>11</sub> H <sub>9</sub> F <sub>2</sub> N <sub>5</sub>
<b>4a</b>	2-(4-Methylthiazol-2-yl)but-3-yn-2-ol	C <sub>8</sub> H <sub>9</sub> NOS
<b>4b</b>	2-(Pyridin-2-yl)but-3-yn-2-ol	C <sub>9</sub> H <sub>9</sub> NO
<b>4c</b>	2-(Pyridin-3-yl)but-3-yn-2-ol	C <sub>9</sub> H <sub>9</sub> NO
<b>4d</b>	2-(Pyridin-4-yl)but-3-yn-2-ol	C <sub>9</sub> H <sub>9</sub> NO
<b>4e</b>	2-(3-Fluoropyridin-2-yl)but-3-yn-2-ol	C <sub>9</sub> H <sub>8</sub> FNO
<b>4f</b>	2-(Pyrazin-2-yl)but-3-yn-2-ol	C <sub>8</sub> H <sub>8</sub> N <sub>2</sub> O

Compd.	Chemical name	Molecular formula
<b>4g</b>	2-(Pyrimidin-2-yl)but-3-yn-2-ol	C <sub>8</sub> H <sub>8</sub> N <sub>2</sub> O
<b>4h</b>	2-(2-Methoxyphenyl)but-3-yn-2-ol	C <sub>11</sub> H <sub>12</sub> O <sub>2</sub>
<b>4i</b>	2-(4-Methoxyphenyl)but-3-yn-2-ol	C <sub>11</sub> H <sub>12</sub> O <sub>2</sub>
<b>4j</b>	2-( <i>m</i> -Tolyl)but-3-yn-2-ol	C <sub>11</sub> H <sub>12</sub> O <sub>2</sub>
<b>4k</b>	2-(Benzo[ <i>d</i> ][1,3]dioxol-5-yl)but-3-yn-2-ol	C <sub>11</sub> H <sub>10</sub> O <sub>3</sub>
<b>4l</b>	2-(4-(Dimethylamino)phenyl)but-3-yn-2-ol	C <sub>12</sub> H <sub>15</sub> NO
<b>4m</b>	2-(5-Bromothiophen-2-yl)but-3-yn-2-ol	C <sub>8</sub> H <sub>7</sub> BrOS
<b>4n</b>	2-(Thiophen-2-yl)but-3-yn-2-ol	C <sub>8</sub> H <sub>8</sub> OS
<b>4o</b>	2-(4-Nitrophenyl)but-3-yn-2-ol	C <sub>10</sub> H <sub>9</sub> NO <sub>3</sub>
<b>4p</b>	2-(2,6-Difluorophenyl)but-3-yn-2-ol	C <sub>10</sub> H <sub>8</sub> F <sub>2</sub> O
<b>5a</b>	1-(1-((1-(2,6-Difluorobenzyl)-1 <i>H</i> -pyrazol-3-yl)methyl)-1 <i>H</i> -1,2,3-triazol-4-yl)-1-(4-methylthiazol-2-yl)ethan-1-ol	C <sub>19</sub> H <sub>18</sub> F <sub>2</sub> N <sub>6</sub> O <sub>2</sub> S
<b>5b</b>	1-(1-((1-(2,6-Difluorobenzyl)-1 <i>H</i> -pyrazol-3-yl)methyl)-1 <i>H</i> -1,2,3-triazol-4-yl)-1-(pyridin-2-yl)ethan-1-ol	C <sub>20</sub> H <sub>18</sub> F <sub>2</sub> N <sub>6</sub> O
<b>5c</b>	1-(1-((1-(2,6-Difluorobenzyl)-1 <i>H</i> -pyrazol-3-yl)methyl)-1 <i>H</i> -1,2,3-triazol-4-yl)-1-(pyridin-3-yl)ethan-1-ol	C <sub>20</sub> H <sub>18</sub> F <sub>2</sub> N <sub>6</sub> O
<b>5d</b>	1-(1-((1-(2,6-Difluorobenzyl)-1 <i>H</i> -pyrazol-3-yl)methyl)-1 <i>H</i> -1,2,3-triazol-4-yl)-1-(pyridin-4-yl)ethan-1-ol	C <sub>20</sub> H <sub>18</sub> F <sub>2</sub> N <sub>6</sub> O <sub>2</sub>
<b>5e</b>	1-(1-((1-(2,6-Difluorobenzyl)-1 <i>H</i> -pyrazol-3-yl)methyl)-1 <i>H</i> -1,2,3-triazol-4-yl)-1-(3-fluoropyridin-2-yl)ethan-1-ol	C <sub>20</sub> H <sub>17</sub> F <sub>3</sub> N <sub>6</sub> O
<b>5f</b>	1-(1-((1-(2,6-Difluorobenzyl)-1 <i>H</i> -pyrazol-3-yl)methyl)-1 <i>H</i> -1,2,3-triazol-4-yl)-1-(pyrazin-2-yl)ethan-1-ol	C <sub>19</sub> H <sub>17</sub> F <sub>2</sub> N <sub>7</sub> O
<b>5g</b>	1-(1-((1-(2,6-Difluorobenzyl)-1 <i>H</i> -pyrazol-3-yl)methyl)-1 <i>H</i> -1,2,3-triazol-4-yl)-1-(pyrimidin-2-yl)ethan-1-ol	C <sub>19</sub> H <sub>17</sub> F <sub>2</sub> N <sub>7</sub> O
<b>5h</b>	1-(1-((1-(2,6-Difluorobenzyl)-1 <i>H</i> -pyrazol-3-yl)methyl)-1 <i>H</i> -1,2,3-triazol-4-yl)-1-(2-methoxyphenyl)ethan-1-ol	C <sub>22</sub> H <sub>21</sub> F <sub>2</sub> N <sub>5</sub> O <sub>2</sub>
<b>5i</b>	1-(1-((1-(2,6-Difluorobenzyl)-1 <i>H</i> -pyrazol-3-yl)methyl)-1 <i>H</i> -1,2,3-triazol-4-yl)-1-(4-methoxyphenyl)ethan-1-ol	C <sub>22</sub> H <sub>21</sub> F <sub>2</sub> N <sub>5</sub> O <sub>2</sub>
<b>5j</b>	1-(1-((1-(2,6-Difluorobenzyl)-1 <i>H</i> -pyrazol-3-yl)methyl)-1 <i>H</i> -1,2,3-triazol-4-yl)-1-( <i>m</i> -tolyl)ethan-1-ol	C <sub>22</sub> H <sub>21</sub> F <sub>2</sub> N <sub>5</sub> O
<b>5k</b>	1-(Benzo[ <i>d</i> ][1,3]dioxol-5-yl)-1-(1-((1-(2,6-difluorobenzyl)-1 <i>H</i> -pyrazol-3-yl)methyl)-1 <i>H</i> -1,2,3-triazol-4-yl)ethan-1-ol	C <sub>22</sub> H <sub>19</sub> F <sub>2</sub> N <sub>5</sub> O <sub>3</sub>
<b>5l</b>	1-(1-((1-(2,6-Difluorobenzyl)-1 <i>H</i> -pyrazol-3-yl)methyl)-1 <i>H</i> -1,2,3-triazol-4-yl)-1-(4-(dimethylamino)phenyl)ethan-1-ol	C <sub>23</sub> H <sub>24</sub> F <sub>2</sub> N <sub>6</sub> O

Compd.	Chemical name	Molecular formula
<b>5m</b>	1-(5-Bromothiophen-2-yl)-1-((1-(2,6-difluorobenzyl)-1H-pyrazol-3-yl)methyl)-1H-1,2,3-triazol-4-yl)ethan-1-ol	C <sub>19</sub> H <sub>16</sub> BrF <sub>2</sub> N <sub>5</sub> OS
<b>5n</b>	1-(1-((1-(2,6-Difluorobenzyl)-1H-pyrazol-3-yl)methyl)-1H-1,2,3-triazol-4-yl)-1-(thiophen-2-yl)ethan-1-ol	C <sub>19</sub> H <sub>17</sub> F <sub>2</sub> N <sub>3</sub> OS
<b>5o</b>	1-(1-((1-(2,6-Difluorobenzyl)-1H-pyrazol-3-yl)methyl)-1H-1,2,3-triazol-4-yl)-1-(4-nitrophenyl)ethan-1-ol	C <sub>21</sub> H <sub>18</sub> F <sub>2</sub> N <sub>6</sub> O <sub>3</sub>
<b>5p</b>	1-(1-((1-(2,6-Difluorobenzyl)-1H-pyrazol-3-yl)methyl)-1H-1,2,3-triazol-4-yl)-1-(2,6-difluorophenyl)ethan-1-ol	C <sub>21</sub> H <sub>17</sub> F <sub>4</sub> N <sub>3</sub> O
<b>6a</b>	2,4-Bis(4-methylthiazol-2-yl)hex-5-yne-2,4-diol	C <sub>14</sub> H <sub>16</sub> N <sub>2</sub> O <sub>2</sub> S <sub>2</sub>
<b>6b</b>	2,4-Di(pyridin-2-yl)hex-5-yne-2,4-diol	C <sub>16</sub> H <sub>16</sub> N <sub>2</sub> O <sub>2</sub>
<b>6c</b>	2,4-bis(3-Fluoropyridin-2-yl)hex-5-yne-2,4-diol	C <sub>16</sub> H <sub>14</sub> FN <sub>2</sub> O <sub>2</sub>
<b>6d</b>	2,4-bis(4-Nitrophenyl)hex-5-yne-2,4-diol	C <sub>18</sub> H <sub>16</sub> N <sub>2</sub> O <sub>6</sub>
<b>6e</b>	2,4-bis(2,6-Difluorophenyl)hex-5-yne-2,4-diol	C <sub>18</sub> H <sub>16</sub> N <sub>2</sub> O <sub>6</sub>
<b>6f</b>	2,4-Bis(3,5-bis(trifluoromethyl)phenyl)hex-5-yne-2,4-diol	C <sub>22</sub> H <sub>14</sub> F <sub>12</sub> O <sub>2</sub>
<b>7</b>	4-(Azidomethyl)-N-((4-(4-phenylthiazol-2-yl)tetrahydro-2H-pyran-4-yl)methyl)benzamide	C <sub>23</sub> H <sub>23</sub> N <sub>5</sub> O <sub>2</sub> S
<b>8a</b>	4-((1H-1,2,3-Triazol-1-yl)methyl)-N-((4-(4-phenylthiazol-2-yl)tetrahydro-2H-pyran-4-yl)methyl)benzamide	C <sub>25</sub> H <sub>25</sub> N <sub>5</sub> O <sub>2</sub> S
<b>8b</b>	4-(((4-(Dimethylamino)methyl)-1H-1,2,3-triazol-1-yl)methyl)-N-((4-(4-phenylthiazol-2-yl)tetrahydro-2H-pyran-4-yl)methyl)benzamide	C <sub>28</sub> H <sub>32</sub> N <sub>6</sub> O <sub>2</sub> S
<b>8c</b>	1-(((4-(4-Phenylthiazol-2-yl)tetrahydro-2H-pyran-4-yl)methyl)-carbamoyl)benzyl)-1H-1,2,3-triazole-4-carboxamide	C <sub>25</sub> H <sub>25</sub> N <sub>5</sub> O <sub>2</sub> S
<b>8d</b>	Ethyl 1-(4-(((4-(4-phenylthiazol-2-yl)tetrahydro-2H-pyran-4-yl)methyl)carbamoyl)benzyl)-1H-1,2,3-triazole-4-carboxylate	C <sub>28</sub> H <sub>29</sub> N <sub>5</sub> O <sub>4</sub> S
<b>8e</b>	1-(4-(((4-(4-Phenylthiazol-2-yl)tetrahydro-2H-pyran-4-yl)methyl)-carbamoyl)benzyl)-1H-1,2,3-triazole-4-carboxylic acid	C <sub>26</sub> H <sub>25</sub> N <sub>5</sub> O <sub>4</sub> S
<b>8f</b>	4-(((4-Cyclopropyl-1H-1,2,3-triazol-1-yl)methyl)-N-((4-(4-phenylthiazol-2-yl)tetrahydro-2H-pyran-4-yl)methyl)benzamide	C <sub>28</sub> H <sub>29</sub> N <sub>5</sub> O <sub>2</sub> S
<b>8g</b>	4-(((4-(3-Methoxyphenyl)-1H-1,2,3-triazol-1-yl)methyl)-N-((4-(4-phenylthiazol-2-yl)tetrahydro-2H-pyran-4-yl)methyl)benzamide	C <sub>32</sub> H <sub>31</sub> N <sub>5</sub> O <sub>3</sub> S
<b>8h</b>	4-((4-Phenyl-1H-1,2,3-triazol-1-yl)methyl)-N-((4-(4-phenylthiazol-2-yl)tetrahydro-2H-pyran-4-yl)methyl)benzamide	C <sub>31</sub> H <sub>29</sub> N <sub>5</sub> O <sub>2</sub> S
<b>8i</b>	N-((4-(4-phenylthiazol-2-yl)tetrahydro-2H-pyran-4-yl)methyl)-4-((4-(pyridin-2-yl)-1H-1,2,3-triazol-1-yl)methyl)benzamide	C <sub>30</sub> H <sub>28</sub> N <sub>6</sub> O <sub>2</sub> S

Table II. Spectral data of compounds 1–8

Compd.	<sup>1</sup> H NMR (400 MHz)	<sup>13</sup> C NMR (101 MHz)	Mass
<b>1</b>	<sup>1</sup> H NMR (400 MHz, Acetone- <i>d</i> <sub>6</sub> ) δ 7.81 (d, <i>J</i> = 2.4 Hz, 1H), 7.47 (tt, <i>J</i> = 8.4, 6.6 Hz, 1H), 7.13–7.01 (m, 2H), 6.75 (d, <i>J</i> = 2.4 Hz, 1H), 5.54 (s, 2H), 4.27 (q, <i>J</i> = 7.1 Hz, 2H), 1.29 (t, <i>J</i> = 7.1 Hz, 3H)	<sup>13</sup> C NMR (101 MHz, Acetone- <i>d</i> <sub>6</sub> ) δ 162.52, 162.36 (dd, <i>J</i> <sub>FC</sub> = 249.4, 7.4 Hz), 144.68, 132.25, 132.15 (t, <i>J</i> <sub>FC</sub> = 10.5 Hz), 112.93 (t, <i>J</i> <sub>FC</sub> = 19.1 Hz), 112.49 (dd, <i>J</i> <sub>FC</sub> = 19.1, 6.2 Hz), 109.35, 60.84, 44.41, 14.58	[M+H] <sup>+</sup> 267.0933 calc. 267.0940
<b>2</b>	<sup>1</sup> H NMR (400 MHz, MeOD) δ 7.58 (d, <i>J</i> = 2.3 Hz, 1H), 7.39 (tt, <i>J</i> = 8.4, 6.5 Hz, 1H), 7.05–6.95 (m, 2H), 6.29 (d, <i>J</i> = 2.3 Hz, 1H), 5.37 (s, 2H), 4.53 (s, 2H)	<sup>13</sup> C NMR (101 MHz, MeOD) δ 162.89 (dd, <i>J</i> <sub>FC</sub> = 249.3, 7.4 Hz), 154.35, 132.30, 132.14 (t, <i>J</i> <sub>FC</sub> = 10.5 Hz), 113.58 (t, <i>J</i> <sub>FC</sub> = 19.1 Hz), 112.61 (dd, <i>J</i> <sub>FC</sub> = 19.2, 6.2 Hz), 105.59, 58.73, 43.64 (t, <i>J</i> <sub>FC</sub> = 3.9 Hz)	[M+H] <sup>+</sup> 225.0828 calc. 225.0834
<b>3</b>	<sup>1</sup> H NMR (400 MHz, Acetone- <i>d</i> <sub>6</sub> ) δ 7.70 (d, <i>J</i> = 2.3 Hz, 1H), 7.44 (tt, <i>J</i> = 8.4, 6.6 Hz, 1H), 7.11–7.00 (m, 2H), 6.29 (d, <i>J</i> = 2.3 Hz, 1H), 5.43 (s, 2H), 4.28 (s, 2H)	<sup>13</sup> C NMR (101 MHz, Acetone- <i>d</i> <sub>6</sub> ) δ 162.42 (dd, <i>J</i> <sub>FC</sub> = 249.1, 7.6 Hz), 147.97, 131.90, 131.83 (t, <i>J</i> <sub>FC</sub> = 10.4 Hz), 113.43 (t, <i>J</i> <sub>FC</sub> = 19.2 Hz), 112.38 (dd, <i>J</i> <sub>FC</sub> = 19.1, 6.3 Hz), 105.81, 48.30, 43.64 (t, <i>J</i> <sub>FC</sub> = 3.7 Hz)	[M+H] <sup>+</sup> 250.0893 calc. 250.0899
<b>4a</b>	<sup>1</sup> H NMR (400 MHz, Acetone- <i>d</i> <sub>6</sub> ) δ 6.92 (dd, <i>J</i> = 2.0, 1.0 Hz, 1H), 5.60 (s, 1H), 2.95 (s, 1H), 2.22 (d, <i>J</i> = 1.0 Hz, 1H), 1.72 (s, 1H)	<sup>13</sup> C NMR (101 MHz, Acetone- <i>d</i> <sub>6</sub> ) δ 175.28, 153.38, 114.92, 87.20, 73.62, 68.80, 31.83, 17.18	[M+H] <sup>+</sup> 168.0478 calc. 168.0478
<b>4b</b>	<sup>1</sup> H NMR (400 MHz, Acetone- <i>d</i> <sub>6</sub> ) δ 8.54 (ddd, <i>J</i> = 4.8, 1.7, 1.0 Hz, 1H), 7.90–7.81 (m, 1H), 7.75 (dt, <i>J</i> = 8.0, 1.1 Hz, 1H), 7.33 (ddd, <i>J</i> = 7.4, 4.8, 1.2 Hz, 1H), 5.51 (s, 1H), 2.98 (s, 1H), 1.76 (s, 3H)	<sup>13</sup> C NMR (101 MHz, Acetone- <i>d</i> <sub>6</sub> ) δ 163.50, 148.70, 138.06, 123.55, 120.40, 88.67, 72.91, 69.52, 31.84	[M+H] <sup>+</sup> 148.0755 calc. 148.0757
<b>4c</b>	<sup>1</sup> H NMR (400 MHz, Acetone- <i>d</i> <sub>6</sub> ) δ 8.87 (dd, <i>J</i> = 2.4, 0.7 Hz, 1H), 8.48 (dd, <i>J</i> = 4.8, 1.6 Hz, 1H), 8.01 (ddd, <i>J</i> = 8.0, 2.4, 1.7 Hz, 1H), 7.36 (ddd, <i>J</i> = 8.0, 4.8, 0.8 Hz, 1H), 5.85 (s, 1H), 3.20 (s, 1H), 1.76 (s, 3H)	<sup>13</sup> C NMR (101 MHz, Acetone- <i>d</i> <sub>6</sub> ) δ 149.17, 147.58, 142.58, 133.48, 123.83, 88.15, 74.19, 67.97, 33.91	[M+H] <sup>+</sup> 148.0756 calc. 148.0757
<b>4d</b>	<sup>1</sup> H NMR (400 MHz, DMSO- <i>d</i> <sub>6</sub> ) δ 8.55 (dd, <i>J</i> = 4.5, 1.6 Hz, 2H), 7.52 (dd, <i>J</i> = 4.5, 1.6 Hz, 2H), 6.41 (s, 1H), 3.59 (s, 1H), 1.62 (s, 3H)	<sup>13</sup> C NMR (101 MHz, DMSO- <i>d</i> <sub>6</sub> ) δ 154.92, 149.57, 120.00, 87.50, 74.83, 67.17, 32.85	[M+H] <sup>+</sup> 148.0757 calc. 148.0757

Compd.	<sup>1</sup> H NMR (400 MHz)	<sup>13</sup> C NMR (101 MHz)	Mass
<b>4e</b>	<sup>1</sup> H NMR (400 MHz, Acetone- <i>d</i> <sub>6</sub> ) δ 8.43 (dt, <i>J</i> = 4.7, 1.5 Hz, 1H), 7.75 (ddd, <i>J</i> = 10.8, 8.3, 1.3 Hz, 1H), 7.56 (ddd, <i>J</i> = 8.3, 4.7, 3.8 Hz, 1H), 5.79 (s, 1H), 3.00 (d, <i>J</i> = 0.7 Hz, 1H), 1.81 (d, <i>J</i> = 1.5 Hz, 3H)	<sup>13</sup> C NMR (101 MHz, Acetone- <i>d</i> <sub>6</sub> ) δ 157.71 (d, <i>J</i> <sub>FC</sub> = 259.4 Hz), 149.62 (d, <i>J</i> <sub>FC</sub> = 13.6 Hz), 144.01 (d, <i>J</i> <sub>FC</sub> = 5.2 Hz), 126.51 (d, <i>J</i> <sub>FC</sub> = 4.1 Hz), 125.89 (d, <i>J</i> <sub>FC</sub> = 19.3 Hz), 86.80 (s), 72.56 (d, <i>J</i> <sub>FC</sub> = 2.2 Hz), 66.62 (d, <i>J</i> <sub>FC</sub> = 5.4 Hz), 29.61 (d, <i>J</i> <sub>FC</sub> = 3.2 Hz)	[M+H] <sup>+</sup> 166.0662 calc. 166.0663
<b>4f</b>	<sup>1</sup> H NMR (400 MHz, Acetone- <i>d</i> <sub>6</sub> ) δ 9.02 (s, 1H), 8.58 (s, 2H), 5.56 (s, 1H), 3.09 (s, 1H), 1.83 (s, 3H)	<sup>13</sup> C NMR (101 MHz, Acetone- <i>d</i> <sub>6</sub> ) δ 159.29, 144.59, 143.95, 142.59, 87.75, 74.02, 69.25, 31.05	[M+H] <sup>+</sup> 149.0709 calc. 149.0709
<b>4g</b>	<sup>1</sup> H NMR (400 MHz, Acetone- <i>d</i> <sub>6</sub> ) δ 8.87 (d, <i>J</i> = 4.9 Hz, 2H), 7.49 (t, <i>J</i> = 4.9 Hz, 1H), 5.29 (s, 1H), 2.94 (s, 1H), 1.82 (s, 3H)	<sup>13</sup> C NMR (101 MHz, Acetone- <i>d</i> <sub>6</sub> ) δ 170.86, 158.30, 121.14, 88.08, 72.82, 70.09, 29.69	[M+H] <sup>+</sup> 149.0707 calc. 149.0709
<b>4h</b>	<sup>1</sup> H NMR (400 MHz, Acetone- <i>d</i> <sub>6</sub> ) δ 7.64 (dd, <i>J</i> = 7.7, 1.7 Hz, 1H), 7.28 (ddd, <i>J</i> = 8.2, 7.4, 1.7 Hz, 1H), 7.04 (dd, <i>J</i> = 8.2, 0.9 Hz, 1H), 6.98–6.92 (m, 1H), 4.88 (s, 1H), 3.90 (s, 3H), 2.88 (s, 1H), 1.80 (s, 3H)	<sup>13</sup> C NMR (101 MHz, Acetone- <i>d</i> <sub>6</sub> ) δ 157.77, 134.14, 129.59, 126.54, 121.15, 112.81, 88.97, 71.51, 68.16, 55.96, 30.47	[M+H] <sup>+</sup> 177.091 calc. 177.0910
<b>4i</b>	<sup>1</sup> H NMR (400 MHz, CDCl <sub>3</sub> ) δ 7.59–7.51 (m, 2H), 6.89–6.82 (m, 2H), 3.77 (s, 3H), 2.89 (s, 1H), 2.65 (s, 1H), 1.75 (s, 3H)	<sup>13</sup> C NMR (101 MHz, Acetone- <i>d</i> <sub>6</sub> ) δ 159.69, 139.13, 126.91, 113.94, 89.23, 73.14, 69.02, 55.44, 34.11	[M+H] <sup>+</sup> 177.091 calc. 177.0910
<b>4j</b>	<sup>1</sup> H NMR (400 MHz, Acetone- <i>d</i> <sub>6</sub> ) δ 7.52–7.49 (m, 1H), 7.48–7.44 (m, 1H), 7.23 (t, <i>J</i> = 7.6 Hz, 1H), 7.12–7.06 (m, 1H), 5.00 (s, 1H), 3.05 (s, 1H), 2.34 (s, 3H), 1.71 (s, 3H)	<sup>13</sup> C NMR (101 MHz, Acetone- <i>d</i> <sub>6</sub> ) δ 147.08, 138.05, 128.63, 128.56, 126.32, 122.80, 89.14, 73.22, 69.34, 34.21, 21.53	[M+H] <sup>+</sup> 161.0958 calc. 161.0961
<b>4k</b>	<sup>1</sup> H NMR (400 MHz, Acetone- <i>d</i> <sub>6</sub> ) δ 7.16 (dd, <i>J</i> = 8.1, 1.7 Hz, 1H), 7.13 (d, <i>J</i> = 1.7 Hz, 1H), 6.79 (d, <i>J</i> = 8.1 Hz, 1H), 5.98 (s, 2H), 5.04 (s, 1H), 3.06 (s, 1H), 1.68 (s, 3H)	<sup>13</sup> C NMR (101 MHz, CDCl <sub>3</sub> ) δ 147.63, 147.13, 139.31, 118.35, 107.88, 106.08, 101.21, 87.39, 73.11, 69.66, 33.20	[M+H] <sup>+</sup> 191.07 calc. 191.0703

Compd.	<sup>1</sup> H NMR (400 MHz)	<sup>13</sup> C NMR (101 MHz)	Mass
<b>4l</b>	<sup>1</sup> H NMR (400 MHz, Acetone- <i>d</i> <sub>6</sub> ) δ 7.51–7.45 (m, 2H), 6.72–6.69 (m, 2H), 4.73 (s, 1H), 3.01 (s, 1H), 2.91 (s, 6H), 1.68 (s, 3H)	<sup>13</sup> C NMR (101 MHz, Acetone- <i>d</i> <sub>6</sub> ) δ 150.91, 134.90, 126.52, 112.75, 89.75, 72.79, 69.09, 40.68, 34.04	[M+H] <sup>+</sup> 190.1223 calc. 190.1226
<b>4m</b>	<sup>1</sup> H NMR (400 MHz, CDCl <sub>3</sub> ) δ 6.94 (d, <i>J</i> = 3.8 Hz, 1H), 6.89 (d, <i>J</i> = 3.8 Hz, 1H), 2.85 (s, 1H), 2.69 (s, 1H), 1.85 (s, 3H)	<sup>13</sup> C NMR (101 MHz, Acetone- <i>d</i> <sub>6</sub> ) δ 154.18, 132.81, 130.47, 124.62, 111.26, 87.49, 73.67, 67.14, 33.93	[M+H] <sup>+</sup> 230.9471 230.9474
<b>4n</b>	<sup>1</sup> H NMR (400 MHz, Acetone- <i>d</i> <sub>6</sub> ) δ 7.33 (dd, <i>J</i> = 5.1, 1.3 Hz, 1H), 7.15 (dd, <i>J</i> = 3.6, 1.3 Hz, 1H), 6.94 (dd, <i>J</i> = 5.1, 3.6 Hz, 1H), 5.37 (s, 1H), 3.12 (s, 1H), 1.82 (s, 3H)	<sup>13</sup> C NMR (101 MHz, Acetone- <i>d</i> <sub>6</sub> ) δ 152.16, 127.09, 125.37, 124.19, 88.31, 73.02, 67.05, 34.27	–
<b>4o</b>	<sup>1</sup> H NMR (400 MHz, Acetone- <i>d</i> <sub>6</sub> ) δ 8.30–8.18 (m, 2H), 8.00–7.86 (m, 2H), 5.50 (s, 1H), 3.21 (s, 1H), 1.75 (s, 3H)	<sup>13</sup> C NMR (101 MHz, Acetone- <i>d</i> <sub>6</sub> ) δ 154.45, 148.14, 127.12, 124.06, 87.88, 74.46, 69.20, 34.01	[M+H] <sup>+</sup> 192.0652 calc. 192.0655
<b>4p</b>	<sup>1</sup> H NMR (400 MHz, Acetone- <i>d</i> <sub>6</sub> ) δ 7.36 (tt, <i>J</i> = 8.3, 6.0 Hz, 1H), 7.02–6.93 (m, 2H), 5.17 (s, 1H), 3.04 (t, <i>J</i> = 0.6 Hz, 1H), 1.94 (t, <i>J</i> = 2.4 Hz, 3H)	<sup>13</sup> C NMR (101 MHz, Acetone- <i>d</i> <sub>6</sub> ) δ 161.22 (dd, <i>J</i> <sub>FC</sub> = 250.6, 7.6 Hz), 130.49 (t, <i>J</i> <sub>FC</sub> = 11.4 Hz), 121.72 (t, <i>J</i> <sub>FC</sub> = 13.4 Hz), 113.77–112.86 (m), 87.86, 72.36 (t, <i>J</i> <sub>FC</sub> = 2.0 Hz), 66.68, 31.77 (t, <i>J</i> <sub>FC</sub> = 4.4 Hz)	[M+H] <sup>+</sup> 183.0615 calc. 183.0616
<b>5a</b>	<sup>1</sup> H NMR (400 MHz, CDCl <sub>3</sub> ) δ 7.59 (s, 1H), 7.40 (d, <i>J</i> = 2.3 Hz, 1H), 7.32 (tt, <i>J</i> = 8.4, 6.5 Hz, 1H), 6.98–6.89 (m, 2H), 6.80 (q, <i>J</i> = 0.9 Hz, 1H), 6.16 (d, <i>J</i> = 2.3 Hz, 1H), 5.47 (s, 2H), 5.35 (s, 2H), 4.88 (s, 1H), 2.38 (d, <i>J</i> = 0.9 Hz, 3H), 2.00 (s, 3H)	<sup>13</sup> C NMR (101 MHz, CDCl <sub>3</sub> ) δ 176.09, 161.50 (dd, <i>J</i> <sub>FC</sub> = 250.6, 7.3 Hz), 152.74, 152.34, 146.12, 130.99, 130.90 (t, <i>J</i> <sub>FC</sub> = 10.4 Hz), 121.02, 114.19, 111.91 (t, <i>J</i> <sub>FC</sub> = 19.1 Hz), 111.73 (dd, <i>J</i> <sub>FC</sub> = 19.2, 6.1 Hz), 105.84, 72.35, 47.92, 43.31 (t, <i>J</i> <sub>FC</sub> = 3.7 Hz), 30.54, 17.17	[M+H] <sup>+</sup> 417.1298 calc. 417.130
<b>5b</b>	<sup>1</sup> H NMR (400 MHz, MeOD) δ 8.47–8.40 (m, 1H), 7.80–7.75 (m, 1H), 7.74 (s, 1H), 7.72–7.67 (m, 1H), 7.60 (d, <i>J</i> = 2.3 Hz, 1H), 7.38 (tt, <i>J</i> = 8.4, 6.6 Hz, 1H), 7.27–7.21 (m, 1H), 7.04–6.94 (m, 2H), 6.23 (d, <i>J</i> = 2.3 Hz, 1H), 5.47 (s, 2H), 5.38 (s, 2H), 1.92 (s, 3H)	<sup>13</sup> C NMR (101 MHz, MeOD) δ 165.53, 162.82 (dd, <i>J</i> <sub>FC</sub> = 249.4, 7.4 Hz), 155.38, 148.93, 148.11, 138.54, 132.85, 132.24 (t, <i>J</i> <sub>FC</sub> = 10.5 Hz), 123.60, 123.16, 121.29, 113.35 (t, <i>J</i> <sub>FC</sub> = 19.1 Hz), 112.62 (dd, <i>J</i> <sub>FC</sub> = 19.2, 6.2 Hz), 73.25, 48.39, 43.94 (t, <i>J</i> <sub>FC</sub> = 3.8 Hz), 29.28	[M+H] <sup>+</sup> 397.1576 calc. 397.1583
<b>5c</b>	<sup>1</sup> H NMR (400 MHz, MeOD) δ 8.68–8.64 (m, 1H), 8.39 (dd, <i>J</i> = 4.9, 1.6 Hz, 1H), 7.92 (ddd, <i>J</i> = 8.1, 2.3, 1.6 Hz, 1H), 7.62 (d, <i>J</i> = 2.3 Hz, 1H), 7.45–7.31 (m, 2H), 7.08–6.95 (m, 2H), 6.24 (d, <i>J</i> = 2.3 Hz, 1H), 5.50 (s, 2H), 5.39 (s, 2H), 1.92 (s, 3H)	<sup>13</sup> C NMR (101 MHz, MeOD) δ 162.85 (dd, <i>J</i> <sub>FC</sub> = 249.4, 7.4 Hz), 155.85, 148.41, 148.11, 147.53, 144.87, 135.50, 132.92, 132.27 (t, <i>J</i> <sub>FC</sub> = 10.5 Hz), 124.69, 122.98, 113.36 (t, <i>J</i> <sub>FC</sub> = 19.1 Hz), 112.64 (d, <i>J</i> <sub>FC</sub> = 19.3, 6.2 Hz), 106.44, 71.43, 48.47, 43.98 (t, <i>J</i> <sub>FC</sub> = 3.9 Hz), 30.63	[M+H] <sup>+</sup> 397.1576 calc. 397.1583

Compd.	<sup>1</sup> H NMR (400 MHz)	<sup>13</sup> C NMR (101 MHz)	Mass
<b>5d</b>	<sup>1</sup> H NMR (400 MHz, MeOD) δ 8.45 (dd, <i>J</i> = 4.6, 1.6 Hz, 2H), 7.77 (s, 1H), 7.62 (d, <i>J</i> = 2.3 Hz, 1H), 7.53 (dd, <i>J</i> = 4.6, 1.7 Hz, 2H), 7.40 (tt, <i>J</i> = 8.4, 6.5 Hz, 1H), 7.05–6.96 (m, 2H), 6.25 (d, <i>J</i> = 2.3 Hz, 1H), 5.50 (s, 2H), 5.39 (s, 2H), 1.89 (s, 3H)	<sup>13</sup> C NMR (101 MHz, MeOD) δ 162.88 (dd, <i>J</i> <sub>FC</sub> = 249.4, 7.4 Hz), 158.89, 155.29, 149.87, 148.10, 132.93, 132.28 (t, <i>J</i> <sub>FC</sub> = 10.5 Hz), 123.11, 122.20, 113.38 (t, <i>J</i> <sub>FC</sub> = 19.1 Hz), 112.64 (dd, <i>J</i> <sub>FC</sub> = 19.3, 6.2 Hz), 106.45, 71.96, 48.47, 43.98, 30.21	[M+H] <sup>+</sup> 397.1575 calc. 397.1583
<b>5e</b>	<sup>1</sup> H NMR (400 MHz, CDCl <sub>3</sub> ) δ 8.36 (dt, <i>J</i> = 4.5, 1.5 Hz, 1H), 7.54 (s, 1H), 7.41 (d, <i>J</i> = 2.2 Hz, 1H), 7.39–7.28 (m, 3H), 6.99–6.90 (m, 2H), 6.29 (s, 1H), 6.15 (d, <i>J</i> = 2.2 Hz, 1H), 5.47 (s, 2H), 5.36 (s, 2H), 1.98 (d, <i>J</i> = 1.8 Hz, 3H)	<sup>13</sup> C NMR (101 MHz, CDCl <sub>3</sub> ) δ 161.51 (dd, <i>J</i> <sub>FC</sub> = 250.5, 7.3 Hz), 156.72 (d, <i>J</i> <sub>FC</sub> = 259.7 Hz), 152.99, 150.17 (d, <i>J</i> <sub>FC</sub> = 14.3 Hz), 146.33, 142.79 (d, <i>J</i> <sub>FC</sub> = 5.1 Hz), 131.00, 130.89 (t, <i>J</i> <sub>FC</sub> = 10.3 Hz), 124.84 (d, <i>J</i> <sub>FC</sub> = 1.8 Hz), 124.73 (d, <i>J</i> <sub>FC</sub> = 13.9 Hz), 120.97, 111.97 (t, <i>J</i> <sub>FC</sub> = 19.1 Hz), 111.73 (dd, <i>J</i> <sub>FC</sub> = 19.4, 6.2 Hz), 105.81, 69.37 (d, <i>J</i> <sub>FC</sub> = 5.5 Hz), 47.84, 43.32 (t, <i>J</i> <sub>FC</sub> = 3.7 Hz), 26.61 (d, <i>J</i> <sub>FC</sub> = 4.0 Hz)	[M+H] <sup>+</sup> 415.1482 calc. 415.1489
<b>5f</b>	<sup>1</sup> H NMR (400 MHz, CDCl <sub>3</sub> ) δ 9.04 (d, <i>J</i> = 1.6 Hz, 1H), 8.51 (d, <i>J</i> = 2.5 Hz, 1H), 8.45 (dd, <i>J</i> = 2.5, 1.6 Hz, 1H), 7.58 (s, 1H), 7.40 (d, <i>J</i> = 2.2 Hz, 1H), 7.33 (tt, <i>J</i> = 8.4, 6.5 Hz, 1H), 7.00–6.90 (m, 2H), 6.17 (d, <i>J</i> = 2.2 Hz, 1H), 5.48 (d, <i>J</i> = 2.1 Hz, 2H), 5.36 (s, 2H), 5.20 (s, 1H), 1.96 (s, 3H)	<sup>13</sup> C NMR (101 MHz, CDCl <sub>3</sub> ) δ 161.58 (dd, <i>J</i> <sub>FC</sub> = 250.6, 7.3 Hz), 158.80, 153.37, 146.16, 143.46, 143.41, 141.91, 131.05, 130.97 (t, <i>J</i> <sub>FC</sub> = 10.4 Hz), 121.05, 111.98 (t, <i>J</i> <sub>FC</sub> = 19.1 Hz), 111.81 (dd, <i>J</i> <sub>FC</sub> = 19.2, 6.1 Hz), 105.92, 71.46, 47.99, 43.41, 30.08	[M+H] <sup>+</sup> 398.1528 calc. 389.1535
<b>5g</b>	<sup>1</sup> H NMR (400 MHz, MeOD) δ 8.77 (d, <i>J</i> = 4.6 Hz, 2H), 7.84 (s, 1H), 7.62 (d, <i>J</i> = 2.2 Hz, 1H), 7.47–7.33 (m, 2H), 7.07–6.97 (m, 2H), 6.25 (d, <i>J</i> = 2.2 Hz, 1H), 5.49 (s, 2H), 5.41 (s, 2H), 1.97 (s, 3H)	<sup>13</sup> C NMR (101 MHz, MeOD) δ 172.86 (bs), 162.83 (dd, <i>J</i> <sub>FC</sub> = 249.4, 7.4 Hz), 158.24 (bs), 155.07 (bs), 148.03, 132.87, 132.25 (t, <i>J</i> <sub>FC</sub> = 10.5 Hz), 123.42 (bs), 121.00 (bs), 113.35 (t, <i>J</i> <sub>FC</sub> = 19.1 Hz), 112.62 (dd, <i>J</i> <sub>FC</sub> = 19.2, 6.2 Hz), 106.48, 74.02, 43.95 (t, <i>J</i> <sub>FC</sub> = 3.8 Hz), 28.25	[M+H] <sup>+</sup> 398.1528 calc. 389.1535
<b>5h</b>	<sup>1</sup> H NMR (400 MHz, CDCl <sub>3</sub> ) δ 7.45 (s, 1H), 7.40 (d, <i>J</i> = 2.2 Hz, 1H), 7.37–7.27 (m, 2H), 7.25–7.19 (m, 1H), 6.98–6.89 (m, 3H), 6.88–6.81 (m, 1H), 6.14 (d, <i>J</i> = 2.2 Hz, 1H), 5.48 (s, 2H), 5.35 (s, 2H), 4.73 (s, 1H), 3.67 (s, 3H), 1.95 (s, 3H)	<sup>13</sup> C NMR (101 MHz, CDCl <sub>3</sub> ) δ 161.45 (dd, <i>J</i> <sub>FC</sub> = 250.6, 7.3 Hz), 156.50, 155.08, 146.54, 133.94, 130.90, 130.88 (t, <i>J</i> <sub>FC</sub> = 10.4 Hz), 128.80, 126.92, 121.05, 120.74, 111.89 (t, <i>J</i> <sub>FC</sub> = 19.0 Hz), 111.69 (dd, <i>J</i> <sub>FC</sub> = 19.1, 6.0 Hz), 111.56, 105.62, 72.35, 55.28, 47.78, 43.27 (t, <i>J</i> <sub>FC</sub> = 3.6 Hz), 28.43	[M+H] <sup>+</sup> 426.1729 calc. 426.1736
<b>5i</b>	<sup>1</sup> H NMR (400 MHz, Acetone- <i>d</i> <sub>6</sub> ) δ 7.67–7.64 (m, 2H), 7.49–7.38 (m, 3H), 7.10–7.00 (m, 2H), 6.87–6.78 (m, 2H), 6.22 (d, <i>J</i> = 2.3 Hz, 1H), 5.45 (s, 2H), 5.41 (s, 2H), 4.90 (s, 1H), 3.74 (s, 3H), 1.89 (s, 3H)	<sup>13</sup> C NMR (101 MHz, Acetone- <i>d</i> <sub>6</sub> ) δ 162.28 (dd, <i>J</i> <sub>FC</sub> = 249.1, 7.6 Hz), 159.15, 156.65, 147.82, 141.20, 132.04, 131.86 (t, <i>J</i> <sub>FC</sub> = 10.5 Hz), 127.27, 121.52, 113.77, 113.28 (t, <i>J</i> <sub>FC</sub> = 19.2 Hz), 112.37 (dd, <i>J</i> <sub>FC</sub> = 19.1, 6.2 Hz), 105.84, 72.07, 55.38, 47.94, 43.59 (t, <i>J</i> <sub>FC</sub> = 3.7 Hz), 31.42	[M+H] <sup>+</sup> 426.1727 calc. 426.1736

Compd.	<sup>1</sup> H NMR (400 MHz)	<sup>13</sup> C NMR (101 MHz)	Mass
<b>5j</b>	<sup>1</sup> H NMR (400 MHz, Acetone- <i>d</i> <sub>6</sub> ) δ 7.68–7.64 (m, 2H), 7.49–7.38 (m, 2H), 7.35–7.31 (m, 1H), 7.15 (dd, <i>J</i> = 9.5, 5.7 Hz, 1H), 7.09–7.03 (m, 2H), 7.02–6.98 (m, 1H), 6.23 (d, <i>J</i> = 2.3 Hz, 1H), 5.45 (s, 2H), 5.41 (s, 2H), 4.80 (s, 1H), 2.28 (s, 3H), 1.89 (s, 3H)	<sup>13</sup> C NMR (101 MHz, Acetone- <i>d</i> <sub>6</sub> ) δ 162.33 (dd, <i>J</i> <sub>FC</sub> = 249.1, 7.6 Hz), 156.41, 149.06, 147.85, 137.76, 132.05, 131.90 (t, <i>J</i> <sub>FC</sub> = 10.5 Hz), 128.44, 127.86, 126.71, 123.23, 121.58, 113.33 (t, <i>J</i> <sub>FC</sub> = 19.2 Hz), 112.40 (dd, <i>J</i> <sub>FC</sub> = 19.1, 6.2 Hz), 105.86, 72.34, 47.96, 43.61 (t, <i>J</i> <sub>FC</sub> = 3.8 Hz), 31.39, 21.59	[M+H] <sup>+</sup> 410.1781 calc. 410.1787
<b>5k</b>	<sup>1</sup> H NMR (400 MHz, Acetone- <i>d</i> <sub>6</sub> ) δ 7.68 (s, 1H), 7.66 (d, <i>J</i> = 2.2 Hz, 1H), 7.44 (t, <i>J</i> = 8.4, 6.6 Hz, 1H), 7.09–7.03 (m, 3H), 7.01 (dd, <i>J</i> = 8.1, 1.8 Hz, 1H), 6.73 (d, <i>J</i> = 8.1 Hz, 1H), 6.23 (d, <i>J</i> = 2.2 Hz, 1H), 5.93 (d, <i>J</i> = 0.5 Hz, 2H), 5.46 (s, 2H), 5.41 (s, 2H), 4.87 (s, 1H), 1.88 (s, 3H)	<sup>13</sup> C NMR (101 MHz, Acetone- <i>d</i> <sub>6</sub> ) δ 162.31 (dd, <i>J</i> <sub>FC</sub> = 249.1, 7.5 Hz), 156.38, 148.08, 147.82, 146.93, 143.34, 132.06, 131.88 (t, <i>J</i> <sub>FC</sub> = 10.5 Hz), 121.54, 119.14, 113.30 (t, <i>J</i> <sub>FC</sub> = 19.2 Hz), 112.39 (dd, <i>J</i> <sub>FC</sub> = 19.1, 6.2 Hz), 108.01, 107.13, 105.87, 101.73, 72.27, 47.97, 43.61 (t, <i>J</i> <sub>FC</sub> = 3.7 Hz), 31.45	[M+H] <sup>+</sup> 440.1522 calc. 440.1529
<b>5l</b>	<sup>1</sup> H NMR (400 MHz, CDCl <sub>3</sub> ) δ 7.39 (d, <i>J</i> = 2.2 Hz, 1H), 7.35 (s, 1H), 7.34–7.27 (m, 3H), 6.98–6.89 (m, 1H), 6.70–6.63 (m, 2H), 6.16 (d, <i>J</i> = 2.2 Hz, 1H), 5.46 (s, 2H), 5.35 (s, 2H), 3.04 (bs, 1), 2.92 (s, 6H), 1.91 (s, 3H)	<sup>13</sup> C NMR (101 MHz, CDCl <sub>3</sub> ) δ 161.57 (dd, <i>J</i> <sub>FC</sub> = 250.7, 7.3 Hz), 155.63, 149.80, 146.42, 134.72, 131.00, 130.93 (t, <i>J</i> <sub>FC</sub> = 10.2 Hz), 126.21, 120.57, 112.31, 112.02 (t, <i>J</i> <sub>FC</sub> = 19.1 Hz), 111.78 (dd, <i>J</i> <sub>FC</sub> = 19.2, 6.1 Hz), 105.83, 71.91, 47.89, 43.38 (t, <i>J</i> <sub>FC</sub> = 3.7 Hz), 40.73, 30.64	[M+H] <sup>+</sup> 439.2045 calc. 439.2052
<b>5m</b>	<sup>1</sup> H NMR (400 MHz, CDCl <sub>3</sub> ) δ 7.47 (s, 1H), 7.41 (d, <i>J</i> = 2.2 Hz, 1H), 7.32 (ddd, <i>J</i> = 14.9, 8.3, 6.6 Hz, 1H), 7.00–6.88 (m, 2H), 6.83 (d, <i>J</i> = 3.8 Hz, 1H), 6.62 (d, <i>J</i> = 3.8 Hz, 1H), 6.17 (d, <i>J</i> = 2.2 Hz, 1H), 5.47 (s, 2H), 5.35 (s, 2H), 4.02 (s, 1H), 1.94 (s, 3H)	<sup>13</sup> C NMR (101 MHz, CDCl <sub>3</sub> ) δ 161.52 (dd, <i>J</i> <sub>FC</sub> = 250.6, 7.3 Hz), 153.79, 153.43, 146.09, 131.07, 130.97 (t, <i>J</i> <sub>FC</sub> = 10.4 Hz), 129.53, 123.87, 120.58, 111.93 (t, <i>J</i> <sub>FC</sub> = 19.1 Hz), 111.77 (dd, <i>J</i> <sub>FC</sub> = 19.1, 6.0 Hz), 111.51, 105.86, 70.83, 47.93, 43.39 (t, <i>J</i> <sub>FC</sub> = 3.5 Hz), 31.07	[M+H] <sup>+</sup> 480.0294 calc. 480.0300
<b>5n</b>	<sup>1</sup> H NMR (400 MHz, Acetone- <i>d</i> <sub>6</sub> ) δ 7.76 (s, 1H), 7.67 (d, <i>J</i> = 2.2 Hz, 1H), 7.44 (t, <i>J</i> = 8.4, 6.6 Hz, 1H), 7.26 (dd, <i>J</i> = 5.0, 1.2 Hz, 1H), 7.10–7.01 (m, 2H), 6.96 (dd, <i>J</i> = 3.5, 1.2 Hz, 1H), 6.90 (dd, <i>J</i> = 5.0, 3.5 Hz, 1H), 6.24 (d, <i>J</i> = 2.2 Hz, 1H), 5.49 (s, 2H), 5.42 (s, 2H), 5.34 (s, 1H), 2.01 (s, 3H)	<sup>13</sup> C NMR (101 MHz, Acetone- <i>d</i> <sub>6</sub> ) δ 162.21 (dd, <i>J</i> <sub>FC</sub> = 249.2, 7.5 Hz), 155.68, 154.20, 147.71, 132.04, 131.84 (t, <i>J</i> <sub>FC</sub> = 10.5 Hz), 127.12, 124.72, 123.85, 121.48, 113.20 (t, <i>J</i> <sub>FC</sub> = 19.3 Hz), 112.33 (d, <i>J</i> <sub>FC</sub> = 19.1, 6.2 Hz), 105.82, 71.26, 47.96, 43.56 (t, <i>J</i> <sub>FC</sub> = 3.7 Hz), 31.89	[M+H] <sup>+</sup> 402.1187 calc. 402.1195
<b>5o</b>	<sup>1</sup> H NMR (400 MHz, Acetone- <i>d</i> <sub>6</sub> ) δ 8.20–8.14 (m, 2H), 7.87–7.80 (m, 2H), 7.75 (s, 1H), 7.67 (d, <i>J</i> = 2.2 Hz, 1H), 7.47 (t, <i>J</i> = 8.4, 6.6 Hz, 1H), 7.12–7.02 (m, 2H), 6.23 (d, <i>J</i> = 2.2 Hz, 1H), 5.47 (s, 2H), 5.41 (s, 2H), 5.20 (s, 1H), 1.93 (s, 3H)	<sup>13</sup> C NMR (101 MHz, Acetone- <i>d</i> <sub>6</sub> ) δ 162.37 (dd, <i>J</i> <sub>FC</sub> = 249.1, 7.5 Hz), 156.45, 155.19, 147.74, 147.59, 132.14, 131.94 (t, <i>J</i> <sub>FC</sub> = 10.5 Hz), 127.44, 123.77, 122.00, 113.36 (t, <i>J</i> <sub>FC</sub> = 19.2 Hz), 112.43 (dd, <i>J</i> <sub>FC</sub> = 19.1, 6.2 Hz), 105.92, 72.40, 48.11, 43.70, 43.66, 43.62, 31.21	[M+H] <sup>+</sup> 441.1473 calc. 441.1481

Compd.	<sup>1</sup> H NMR (400 MHz)	<sup>13</sup> C NMR (101 MHz)	Mass
<b>5p</b>	<sup>1</sup> H NMR (400 MHz, DMSO- <i>d</i> <sub>6</sub> ) δ 7.90 (s, 1H), 7.77 (d, <i>J</i> = 2.2 Hz, 1H), 7.47 (tt, <i>J</i> = 8.4, 6.7 Hz, 1H), 7.32 (tt, <i>J</i> = 8.3, 6.0 Hz, 1H), 7.20–7.08 (m, 2H), 7.02–6.89 (m, 2H), 6.15 (d, <i>J</i> = 2.2 Hz, 1H), 5.94 (bs, 1H), 5.46 (s, 2H), 5.37 (s, 2H), 1.90 (t, <i>J</i> = 2.6 Hz, 3H)	<sup>13</sup> C NMR (101 MHz, DMSO- <i>d</i> <sub>6</sub> ) δ 160.94 (dd, <i>J</i> <sub>FC</sub> = 248.8, 7.7 Hz), 160.34 (dd, <i>J</i> <sub>FC</sub> = 249.9, 8.4 Hz), 154.81, 147.02, 131.85, 131.17 (t, <i>J</i> <sub>FC</sub> = 10.4 Hz), 129.35 (t, <i>J</i> <sub>FC</sub> = 11.5 Hz), 122.28 (t, <i>J</i> <sub>FC</sub> = 13.6 Hz), 120.83, 112.48 (dd, <i>J</i> <sub>FC</sub> = 20.4, 7.3 Hz), 112.32 (t, <i>J</i> <sub>FC</sub> = 19.2 Hz), 111.82 (dd, <i>J</i> <sub>FC</sub> = 18.8, 6.0 Hz), 104.82, 70.10, 46.86, 42.63 (t, <i>J</i> <sub>FC</sub> = 3.4 Hz), 30.60 (t, <i>J</i> <sub>FC</sub> = 4.8 Hz)	[M+H] <sup>+</sup> 432.1435 calc. 432.1442
<b>6a</b>	<sup>1</sup> H NMR (400 MHz, CDCl <sub>3</sub> ) δ 7.25 (s, 1H), 7.22 (s, 0.8H), 6.81 (q, <i>J</i> = 0.9 Hz, 1H), 6.79 (q, <i>J</i> = 0.9 Hz, 0.8H), 6.77–6.74 (m, 1.8H), 6.39 (bs, 1H), 5.79 (bs, 0.8H), 3.13 (d, <i>J</i> = 15.2 Hz, 1H), 3.05 (d, <i>J</i> = 15.0 Hz, 0.8H), 2.95 (d, <i>J</i> = 15.2 Hz, 1H), 2.94 (d, <i>J</i> = 15.0 Hz, 0.8H), 2.68 (s, 0.8H), 2.49 (s, 1H), 2.39 (d, <i>J</i> = 0.9 Hz, 3H), 2.37 (d, <i>J</i> = 0.9 Hz, 3H), 2.36 (d, <i>J</i> = 0.9 Hz, 2.4H), 2.33 (d, <i>J</i> = 0.9 Hz, 2.4H), 1.70 (s, 2.4H), 1.65 (s, 3H)	<sup>13</sup> C NMR (101 MHz, CDCl <sub>3</sub> ) δ 179.30, 178.84, 174.87, 174.05, 152.48, 152.36, 151.70, 151.61, 114.93, 114.50, 113.96, 113.90, 84.84, 83.91, 75.57, 75.45, 75.20, 74.45, 70.56, 70.20, 53.42, 52.95, 32.49, 31.94, 17.06, 17.00, 16.95, 16.86	[M+H] <sup>+</sup> 309.072 calc. 309.0726
<b>6b</b>	<sup>1</sup> H NMR (400 MHz, CDCl <sub>3</sub> ) δ 8.32–8.29 (m, 1H), 8.25–8.22 (m, 1H), 7.55–7.45 (m, 3H), 7.31–7.25 (m, 1H), 7.05–6.95 (m, 2H), 2.94 (d, <i>J</i> = 14.8 Hz, 1H), 2.77 (d, <i>J</i> = 14.8 Hz, 1H), 2.62 (s, 1H), 1.69 (s, 3H)	<sup>13</sup> C NMR (101 MHz, CDCl <sub>3</sub> ) δ 164.26, 161.20, 147.66, 147.07, 136.82, 136.70, 122.27, 121.57, 120.20, 119.67, 87.32, 75.59, 72.94, 72.09, 51.15, 30.98	[M+H] <sup>+</sup> 269.1279 calc. 269.1285
<b>6c</b>	<sup>1</sup> H NMR (400 MHz, CDCl <sub>3</sub> ) δ 8.19–8.10 (m, 2H), 7.30–7.07 (m, 4H), 6.18 (s, 1H), 5.79 (s, 1H), 3.03–2.92 (m, 2H), 2.55 (d, <i>J</i> = 0.7 Hz, 1H), 1.62 (d, <i>J</i> = 1.6 Hz, 3H)	<sup>13</sup> C NMR (101 MHz, CDCl <sub>3</sub> ) δ 156.69 (d, <i>J</i> <sub>FC</sub> = 261.2 Hz), 156.51 (d, <i>J</i> <sub>FC</sub> = 257.9 Hz), 151.26 (d, <i>J</i> <sub>FC</sub> = 14.3 Hz), 147.55 (d, <i>J</i> <sub>FC</sub> = 12.8 Hz), 143.00 (d, <i>J</i> <sub>FC</sub> = 5.1 Hz), 142.88 (d, <i>J</i> <sub>FC</sub> = 5.1 Hz), 124.71 (d, <i>J</i> <sub>FC</sub> = 3.7 Hz), 124.06 (d, <i>J</i> <sub>FC</sub> = 19.5 Hz), 123.93 (d, <i>J</i> <sub>FC</sub> = 3.9 Hz), 123.74 (d, <i>J</i> <sub>FC</sub> = 20.3 Hz), 85.12, 73.18 (d, <i>J</i> <sub>FC</sub> = 6.2 Hz), 72.20 (d, <i>J</i> <sub>FC</sub> = 2.6 Hz), 69.01 (d, <i>J</i> <sub>FC</sub> = 5.9 Hz), 48.60 (t, <i>J</i> <sub>FC</sub> = 2.8 Hz), 28.90 (d, <i>J</i> <sub>FC</sub> = 3.7 Hz)	[M+H] <sup>+</sup> 305.1089 calc. 305.1096
<b>6d</b>	<sup>1</sup> H NMR (400 MHz, CDCl <sub>3</sub> ) δ 8.14–8.03 (m, 4H), 7.75–7.66 (m, 2H), 7.57–7.47 (m, 2H), 4.48 (s, 1H), 3.60 (s, 1H), 2.89 (s, 1H), 2.48 (d, <i>J</i> = 15.0 Hz, 1H), 2.38 (d, <i>J</i> = 15.0 Hz, 1H), 1.95 (s, 3H)	<sup>13</sup> C NMR (101 MHz, CDCl <sub>3</sub> ) δ 155.09, 151.58, 147.39, 146.79, 126.38, 125.69, 123.48, 123.47, 85.87, 76.35, 76.01, 72.01, 54.69, 30.52	[M+H] <sup>+</sup> 357.1077 calc. 357.1081

Compd.	<sup>1</sup> H NMR (400 MHz)	<sup>13</sup> C NMR (101 MHz)	Mass
<b>6e</b>	<sup>1</sup> H NMR (400 MHz, CDCl <sub>3</sub> ) δ 7.01–6.85 (m, 2H), 6.61–6.47 (m, 4H), 4.70 (t, <i>J</i> = 3.0 Hz, 1H), 4.29 (t, <i>J</i> = 5.1 Hz, 1H), 3.36 (d, <i>J</i> = 15.2 Hz, 1H), 2.73 (d, <i>J</i> = 15.2 Hz, 1H), 2.62 (s, 1H), 1.69 (s, 3H)	<sup>13</sup> C NMR (101 MHz, CDCl <sub>3</sub> ) δ 159.97 (dd, <i>J</i> <sub>FC</sub> = 247.3, 8.2 Hz), 159.90 (dd, <i>J</i> <sub>FC</sub> = 249.9, 6.9 Hz), 129.22 (t, <i>J</i> <sub>FC</sub> = 11.4 Hz), 128.43 (t, <i>J</i> <sub>FC</sub> = 11.9 Hz), 120.59 (t, <i>J</i> <sub>FC</sub> = 12.5 Hz), 118.02 (t, <i>J</i> <sub>FC</sub> = 11.7 Hz), 112.45 (d, <i>J</i> <sub>FC</sub> = 6.2 Hz), 112.16 (d, <i>J</i> <sub>FC</sub> = 4.8 Hz), 85.78, 76.21 (t, <i>J</i> <sub>FC</sub> = 2.4 Hz), 72.05 (t, <i>J</i> <sub>FC</sub> = 2.1 Hz), 71.11 (t, <i>J</i> <sub>FC</sub> = 1.4 Hz), 50.59 (qui, <i>J</i> <sub>FC</sub> = 2.6 Hz), 32.06 (t, <i>J</i> <sub>FC</sub> = 3.1 Hz)	[M+H] <sup>+</sup> 377.0555 calc. 377.0562
	<sup>1</sup> H NMR (400 MHz, DMSO- <i>d</i> <sub>6</sub> ) δ 7.76 (apps, 2H), 7.73 (apps, 1H), 7.70 (apps, 2H), 7.62 (apps, 1H), 7.07 (s, 1H), 5.94 (s, 1H), 3.66 (s, 1H), 3.16 (d, <i>J</i> = 15.0 Hz, 1H), 2.74 (d, <i>J</i> = 15.0 Hz, 1H), 1.46 (s, 3H)	<sup>13</sup> C NMR (101 MHz, DMSO- <i>d</i> <sub>6</sub> ) δ 150.48, 147.50, 129.52 (q, <i>J</i> <sub>FC</sub> = 32.7 Hz), 129.47 (q, <i>J</i> <sub>FC</sub> = 32.5 Hz), 126.15 (q, <i>J</i> <sub>FC</sub> = 2.7 Hz), 125.89 (q, <i>J</i> <sub>FC</sub> = 2.6 Hz), 123.27 (sek, <i>J</i> <sub>FC</sub> = 2.74 Hz), 123.10 (sek, <i>J</i> <sub>FC</sub> = 2.74 Hz), 120.73 (sek, <i>J</i> <sub>FC</sub> = 3.5 Hz), 119.68 (sek, <i>J</i> <sub>FC</sub> = 3.5 Hz), 87.12, 76.13, 73.68, 70.45, 53.46, 32.78	[M-H] <sup>-</sup> 537.0727 calc. 537.0729
<b>7</b>	<sup>1</sup> H NMR (400 MHz, CDCl <sub>3</sub> ) δ 7.95–7.90 (m, 2H), 7.83–7.78 (m, 2H), 7.52 (s, 1H), 7.51–4.3 (m, 3H), 7.42–7.37 (m, 1H), 7.34–7.29 (m, 2H), 4.38 (s, 2H), 4.00–3.90 (m, 2H), 3.85 (d, <i>J</i> = 5.7 Hz, 2H), 3.78–3.69 (m, 2H), 2.30–2.24 (m, 2H), 2.10–1.98 (m, 2H)	<sup>13</sup> C NMR (101 MHz, CDCl <sub>3</sub> ) δ 176.15, 166.77, 155.14, 138.85, 134.27, 134.05, 128.79, 128.39, 128.08, 127.48, 126.19, 112.60, 63.94, 54.08, 47.52, 42.91, 34.65	[M+H] <sup>+</sup> 434.1647 calc. 434.1645
	<sup>1</sup> H NMR (400 MHz, CDCl <sub>3</sub> ) δ 7.90–7.85 (m, 2H), 7.79–7.75 (m, 2H), 7.71 (d, <i>J</i> = 0.9 Hz, 1H), 7.55 (t, <i>J</i> = 5.6 Hz, 1H), 7.51 (s, 1H), 7.49 (d, <i>J</i> = 0.9 Hz, 1H), 7.44–7.36 (m, 3H), 7.23–7.18 (m, 2H), 5.57 (s, 2H), 3.96–3.86 (m, 2H), 3.80 (d, <i>J</i> = 5.6 Hz, 2H), 3.73–3.64 (m, 2H), 2.32–2.22 (m, 2H), 2.03–1.94 (m, 2H)	<sup>13</sup> C NMR (101 MHz, CDCl <sub>3</sub> ) δ 176.22, 166.65, 155.25, 138.21, 134.84, 134.38, 134.07, 128.88, 128.56, 127.97, 127.82, 126.25, 123.54, 112.69, 64.04, 53.40, 47.62, 42.95, 34.76	[M+H] <sup>+</sup> 460.1802 calc. 460.1802
<b>8a</b>	<sup>1</sup> H NMR (400 MHz, CDCl <sub>3</sub> ) δ 7.94–7.87 (m, 2H), 7.81–7.75 (m, 2H), 7.57 (s, 1H), 7.52 (s, 1H), 7.49 (t, <i>J</i> = 5.7 Hz, 1H), 7.45–7.35 (m, 3H), 7.27–7.22 (m, 2H), 5.55 (s, 2H), 3.99–3.89 (m, 2H), 3.83 (d, <i>J</i> = 5.7 Hz, 2H), 3.76–3.67 (m, 2H), 3.71 (s, 2H), 2.34 (s, 6H), 2.33–2.24 (m, 2H), 2.06–1.96 (m, 2H)	<sup>13</sup> C NMR (101 MHz, CDCl <sub>3</sub> ) δ 176.45, 166.62, 155.35, 144.44, 138.12, 134.93, 134.14, 128.96, 128.65, 128.19, 127.89, 126.32, 123.34, 112.71, 64.11, 54.09, 53.74, 47.51, 44.74, 42.96, 34.86	[M+H] <sup>+</sup> 517.2385 calc. 517.2380
	<sup>1</sup> H NMR (400 MHz, DMSO) δ 8.62 (s, 1H), 8.47 (t, <i>J</i> = 6.4 Hz, 1H), 8.06 (s, 1H), 7.95–7.90 (m, 2H), 7.88 (s, 1H), 7.80–7.73 (d, <i>J</i> = 8.3 Hz, 2H), 7.49 (s, 1H), 7.43–7.28 (m, 5H), 5.69 (s, 2H), 3.88–3.74 (m, 2H), 3.53 (d, <i>J</i> = 6.4 Hz, 2H), 3.45–3.33 (m, 2H), 2.26–2.14 (m, 2H), 2.01–1.88 (m, 2H)	<sup>13</sup> C NMR (101 MHz, DMSO) δ 174.19, 166.35, 161.42, 153.74, 143.19, 138.65, 134.50, 134.34, 128.67, 127.85, 127.76, 126.84, 125.99, 114.38, 63.56, 52.62, 49.35, 44.08, 34.17	[M+H] <sup>+</sup> 503.1862 calc. 503.1860

Compd.	<sup>1</sup> H NMR (400 MHz)	<sup>13</sup> C NMR (101 MHz)	Mass
<b>8d</b>	<sup>1</sup> H NMR (400 MHz, CDCl <sub>3</sub> ) δ 7.98 (s, 1H), 7.91–7.86 (m, 2H), 7.83–7.77 (m, 2H), 7.54 (t, <i>J</i> = 5.6 Hz, 1H), 7.51 (s, 1H), 7.44–7.35 (m, 3H), 7.26–7.22 (m, 2H), 5.60 (s, 2H), 4.40 (q, <i>J</i> = 7.2 Hz, 2H), 3.98–3.87 (m, 2H), 3.82 (d, <i>J</i> = 5.6 Hz, 2H), 3.75–3.66 (m, 2H), 2.35–2.23 (m, 2H), 2.07–1.96 (m, 2H), 1.38 (t, <i>J</i> = 7.2 Hz, 3H)	<sup>13</sup> C NMR (101 MHz, CDCl <sub>3</sub> ) δ 176.36, 166.49, 160.62, 155.34, 140.88, 137.23, 135.30, 134.10, 128.95, 128.67, 128.30, 128.06, 127.45, 126.31, 112.73, 64.10, 61.47, 53.97, 47.60, 42.94, 34.85, 14.39	[M+Na] <sup>+</sup> 594.1855 calc. 554.1852
	<sup>1</sup> H NMR (400 MHz, CDCl <sub>3</sub> ) δ 8.34 (bs, 1H), 8.06 (s, 1H), 7.88–7.82 (m, 2H), 7.80–7.74 (m, 2H), 7.65 (t, <i>J</i> = 5.5 Hz, 1H), 7.49 (s, 1H), 7.42–7.31 (m, 3H), 7.25–7.19 (m, 2H), 5.57 (s, 2H), 3.98–3.87 (m, 2H), 3.81 (d, <i>J</i> = 5.5 Hz, 2H), 3.75–3.63 (m, 2H), 2.34–2.20 (m, 2H), 2.04–1.92 (m, 2H)	<sup>13</sup> C NMR (101 MHz, CDCl <sub>3</sub> ) δ 176.16, 167.05, 162.86, 155.36, 140.22, 137.26, 135.11, 134.10, 128.97, 128.69, 128.40, 128.16, 126.35, 112.86, 64.12, 54.04, 47.89, 42.99, 34.78	[M-H] <sup>-</sup> 502.1564 calc. 502.1554
<b>8e</b>	<sup>1</sup> H NMR (400 MHz, CDCl <sub>3</sub> ) δ 7.92–7.86 (m, 2H), 7.81–7.74 (m, 2H), 7.54 (t, <i>J</i> = 5.7 Hz, 1H), 7.51 (s, 1H), 7.45–7.35 (m, 3H), 7.24–7.18 (m, 2H), 7.15 (s, 1H), 5.48 (s, 2H), 3.97–3.88 (m, 2H), 3.82 (d, <i>J</i> = 5.7 Hz, 2H), 3.75–3.66 (m, 2H), 2.33–2.23 (m, 2H), 2.04–1.97 (m, 2H), 1.96–1.88 (m, 1H), 0.97–0.90 (m, 2H), 0.85–0.79 (m, 2H)	<sup>13</sup> C NMR (101 MHz, CDCl <sub>3</sub> ) δ 176.35, 166.69, 155.32, 150.93, 138.45, 134.80, 134.09, 128.93, 128.62, 128.01, 127.80, 126.29, 119.74, 112.69, 64.07, 53.52, 47.53, 42.93, 34.81, 14.27, 7.88, 6.77	[M+H] <sup>+</sup> 500.2116 calc. 500.2115
	<sup>1</sup> H NMR (400 MHz, CDCl <sub>3</sub> ) δ 7.89–7.84 (m, 2H), 7.82–7.76 (m, 2H), 7.66 (s, 1H), 7.53 (t, <i>J</i> = 5.6 Hz, 1H), 7.49 (s, 1H), 7.43–7.41 (m, 1H), 7.40–7.34 (m, 2H), 7.34–7.23 (m, 5H), 6.92–6.83 (m, 1H), 5.58 (s, 2H), 3.96–3.88 (m, 2H), 3.84 (s, 3H), 3.81 (d, <i>J</i> = 5.6 Hz, 2H), 3.74–3.66 (m, 2H), 2.32–2.23 (m, 2H), 2.04–1.96 (m, 2H)	<sup>13</sup> C NMR (101 MHz, CDCl <sub>3</sub> ) δ 176.30, 166.66, 160.11, 155.32, 148.33, 138.22, 134.97, 134.06, 131.73, 129.97, 128.91, 128.62, 128.04, 127.90, 126.27, 119.86, 118.17, 114.46, 112.68, 110.81, 64.08, 55.43, 53.71, 47.60, 42.93, 34.81	[M+H] <sup>+</sup> 566.2221 calc. 566.2220
<b>8g</b>	<sup>1</sup> H NMR (400 MHz, CDCl <sub>3</sub> ) δ 7.88–7.83 (m, 2H), 7.81–7.75 (m, 2H), 7.68 (s, 1H), 7.55 (t, <i>J</i> = 5.6 Hz, 1H), 7.48 (s, 1H), 7.42–7.20 (m, 8H), 5.56 (s, 2H), 3.95–3.85 (m, 2H), 3.79 (d, <i>J</i> = 5.6 Hz, 1H), 3.72–3.62 (m, 2H), 2.32–2.21 (m, 2H), 2.03–1.93 (m, 2H)	<sup>13</sup> C NMR (101 MHz, CDCl <sub>3</sub> ) δ 176.14, 166.65, 155.23, 148.35, 138.22, 134.88, 134.01, 130.38, 128.87, 128.83, 128.52, 128.31, 127.93, 127.84, 126.20, 125.70, 119.70, 112.66, 64.02, 53.60, 47.65, 42.93, 34.73	[M+H] <sup>+</sup> 536.2118 calc. 536.2115
	<sup>1</sup> H NMR (400 MHz, CDCl <sub>3</sub> ) δ 8.53 (apps, 1H), 8.22–8.13 (m, 1H), 8.08 (s, 1H), 7.90–7.84 (m, 2H), 7.82–7.73 (m, 3H), 7.53 (t, <i>J</i> = 5.4 Hz, 1H), 7.49 (s, 1H), 7.42–7.34 (m, 2H), 7.32–7.25 (m, 3H), 7.25–7.18 (m, 1H), 5.60 (s, 2H), 3.96–3.87 (m, 2H), 3.81 (d, <i>J</i> = 5.7 Hz, 2H), 3.75–3.65 (m, 2H), 2.33–2.23 (m, 2H), 2.04–1.96 (m, 2H)	<sup>13</sup> C NMR (101 MHz, CDCl <sub>3</sub> ) δ 176.26, 166.59, 155.30, 150.04, 149.37, 148.88, 137.90, 137.07, 134.96, 134.06, 128.89, 128.55, 128.24, 127.90, 126.26, 123.05, 122.18, 120.30, 112.66, 64.07, 53.83, 47.59, 42.95, 34.79	[M+H] <sup>+</sup> 537.207 calc. 537.2067

### *Crystallisation and X-ray diffraction*

Crystals of compounds **6c** and **6e** spontaneously formed from the oily residue remaining after the initial workup of the reaction mixture, without the need for any specific crystallisation procedure. Single crystal X-ray diffraction data for **6c** and **6e** were collected at 150 K on a SuperNova diffractometer with an Atlas detector using CrysAlis software with monochromated Mo K $\alpha$  (0.71073 Å) radiation (37). The initial structural models were solved with direct methods implemented in SHELXT using the Olex2 graphical user interface (38). A full-matrix least-squares refinement on F2 magnitudes with anisotropic displacement parameters for all non-hydrogen atoms using Olex2 or SHELXL-2018/3 was performed (38, 39). All non-hydrogen atoms were refined anisotropically, while hydrogen atoms were placed at calculated positions and treated as riding on their parent atoms, except for O-H atoms, which were located in the difference Fourier map and their positions and isotropic displacement parameters were refined. Mercury was used for the preparation of all figures (39, 40). CCDC deposition numbers 2425328–2425329 contain the supplementary crystallographic data for compounds **6c** and **6e** included in this paper, respectively.

### *InhA enzymatic assay*

The activity of compounds was measured fluorimetrically by following NADH oxidation at  $\lambda_{\text{exc}} = 340$  nm and  $\lambda_{\text{em}} = 480$  nm for 10 min at 25 °C. Stock solutions (10 mmol L<sup>-1</sup>) of all compounds were prepared in DMSO, and the final concentration of DMSO in the assay mixture was 1 % V/V. Reactions were initiated by the addition of InhA (60 nmol L<sup>-1</sup>) to solutions containing the inhibitor (100  $\mu\text{mol L}^{-1}$ ), 2-trans-dodecenoyl-coenzyme A (DD-CoA, 50  $\mu\text{mol L}^{-1}$ ), and NADH (100  $\mu\text{mol L}^{-1}$ ) in 30 mmol L<sup>-1</sup> PIPES, pH 6.8. All compounds were soluble under the conditions of the assay. Control reactions were carried out under the same conditions but without the inhibitor and with 1 % V/V DMSO. The inhibitory activity of each compound was expressed as the percentage of InhA activity inhibition relative to the control reaction without the inhibitor. The  $IC_{50}$  value of **5a** was determined at seven different concentrations of inhibitor in the same conditions as described above. The resulting data were analysed using the GraphPad Prism software.

### *Docking experiments*

*Preparation of the Grid Box.* – Grid boxes enclosing the native ligands in the X-ray crystal structures with PDB IDs 5OIT and 4QBP were prepared in Maestro (41) with dimensions similar to those of the workspace ligand. Tyr158 was set as a rotatable residue; however, no constraints were applied during the process.

*Preparation of ligands.* – Molecules were drawn using ChemDraw 18 (PerkinElmer, USA), and OpenBabel 3.1.1(42) was used to convert the structures to SMILES format. These structures were subsequently imported into the Maestro program and prepared using LigPrep from the Schrödinger Suite (41). The conformations of the molecules were generated using the OPLS4 force field and ionised with Epik at a target pH of  $7 \pm 2$ . The conformers were stored in Maestro format for subsequent docking studies.

*Preparation of proteins.* – Protein structures were prepared using the Protein Preparation Wizard implemented in the Schrödinger Suite in Maestro (41). Water molecules, except for those associated with the NADPH cofactor, were removed. Bond orders were auto-

matically assigned, hydrogens were added, selenomethionines were converted to methionines, and missing side chains were added. Native ligands were removed, disulfide bridges were created where applicable, and waters beyond a 5 Å radius of heteroatoms were removed. Heteroatoms were protonated to mimic a pH of 7.0. The Impref utility was then used to perform constrained minimisation of the protein with a maximum root-mean-square deviation (RMSD) of 0.30 Å.

*Docking procedure.* – Docking simulations were carried out using Glide (43) from the Schrödinger Suite in extra precision (XP) mode. Compounds were docked into the predefined grid boxes. To soften the potential for nonpolar regions of the ligand, the van der Waals radii of ligand atoms were scaled using a scaling factor of 0.8, and the partial atomic charges were scaled with a cutoff of 0.15. Flexible ligand sampling and ring conformation sampling were enabled. Epik state penalties were incorporated into the docking scores, intramolecular hydrogen bonds were rewarded, and conjugated  $\pi$ -groups were assigned enhanced planarity. Post-docking minimisation was performed with strain correction terms applied, and no constraints were enforced during docking.

*Visualisation of results.* – Docking poses were analysed and visualised using Schrödinger's Maestro. The original ligand coordinates were used as references to compare the binding positions of the docked m (41) and further prepared using LigPrep (44) from the Schrödinger Suite. The conformations of the molecules were generated using the OPLS4 force field and ionised using Epik (45) at a target pH of  $7 \pm 2$ . The conformers were finally stored in Maestro format for further docking.

## RESULTS AND DISCUSSION

### *Design and synthesis*

In our previous efforts, we explored the chemical space of thiadiazole- and tetrahydropyran-based InhA inhibitors by systematically introducing small structural modifications and evaluating their effects on inhibitory activity (21). However, this approach was time-consuming, as the synthesis of each compound required a linear, multi-step synthesis. To accelerate the synthesis of these compounds, we employed click chemistry, specifically copper-catalysed azide-alkyne cycloaddition (CuAAC). In this design strategy, the left-hand side of the molecule, responsible for interacting with the lipophilic region of the active site, was retained as a constant, whereas the right-hand side, which forms a network of hydrogen bonds, was systematically varied. For compounds based on the thiadiazole lead, the thiadiazole moiety was replaced with a triazole ring (Fig. 2), formed *via* CuAAC between an azide group incorporated into the constant left-hand side and an alkyne moiety introduced into the variable right-hand side. Similarly, for compounds based on the tetrahydropyran lead, the pyrazole moiety was substituted with a triazole ring, generated through the reaction of an azide group on the constant left-hand side and an alkyne moiety on the variable right-hand side.

### *Synthesis of compounds based on the thiadiazol lead compound*

The synthesis of compounds based on the thiadiazole inhibitor began with the preparation of the left-hand-side azide (Scheme 1A). The process started with the reaction of

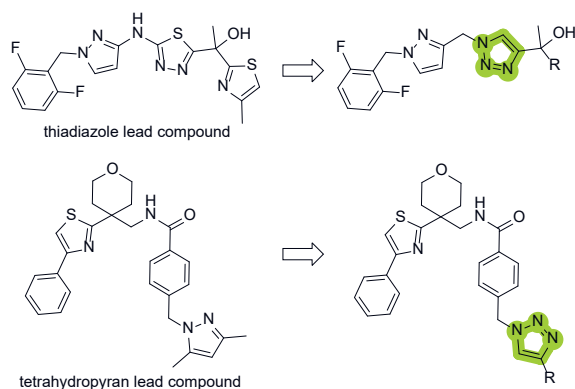


Fig. 2. Thiaziazole and tetrahydropyran lead compounds (left) and the proposed analogues featuring the highlighted 1,2,3-triazole (right).

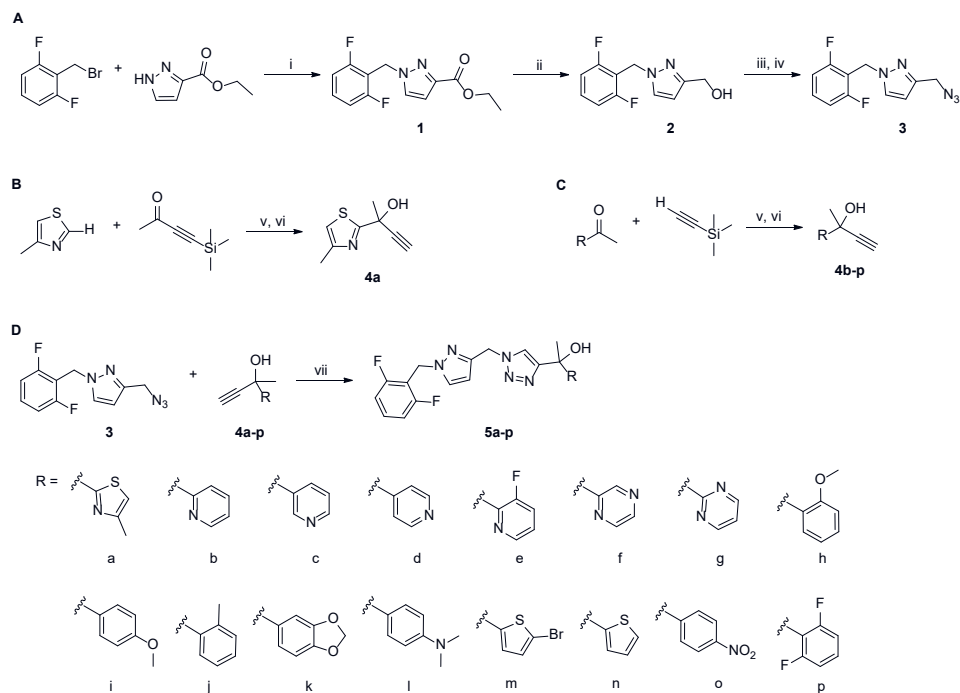
ethyl 1*H*-pyrazole-3-carboxylate with 2-(bromomethyl)-1,3-difluorobenzene in the presence of the strong base sodium hydride (NaH), yielding compound **1**. Subsequently, the ethyl ester group in compound **1** was reduced to an alcohol (compound **2**) using *in situ*-generated borane. In the next step, alcohol **2** was converted to the corresponding mesylate *via* reaction with mesyl chloride. The mesyl ester was then treated with sodium azide to produce the left-hand-side azide **3**.

For the synthesis of the right-hand-side alkynes, several strategies were explored. Thiazole **4a** was synthesised by deprotonating methylthiazole at the 2-position using *n*-BuLi, followed by the reaction of the resulting methylthiazole anion with the carbonyl group of 4-(trimethylsilyl)but-3-yn-2-one. The final step involved the removal of the trimethylsilyl group using tetrabutylammonium fluoride, yielding thiazole **4a** (Scheme 1B).

Attempts to prepare other alkynes initially involved the addition of ethynylmagnesium bromide (a Grignard reagent) to ketones. However, these reactions produced a mixture of products, with 1,3-diols being the major components. This reaction is further discussed in the section *Synthesis of 1,3-diols*. The successful strategy involved the deprotonation of ethynyltrimethylsilane with *n*-BuLi, followed by the addition of the appropriate ketone to generate the desired product. The trimethylsilyl group was then cleaved with TBAF in the final step to produce the alkynes **4b–p** (Scheme 1C). CuAAC between the synthesised azide **3** and alkynes **4a–p** was performed in DCM, using tris(triphenylphosphine)copper(I) bromide or copper(I) bromide as the catalysts to produce the final products **5a–p** (Scheme 1D).

### *Synthesis of 1,3-diols*

As described in the previous chapter, initial attempts to synthesise alkynes **4b**, **4e**, and **4p** *via* the addition of ethynylmagnesium bromide to the corresponding aryl methyl ketones predominantly yielded 1,3-diols as the major products (Scheme 2). To further investigate this unexpected outcome, various reaction parameters were explored, including temperature (0 °C and –80 °C), the equivalents of ethynylmagnesium bromide (1 or 2 equiv), and the choice of aryl methyl ketones. The results indicated that higher reaction

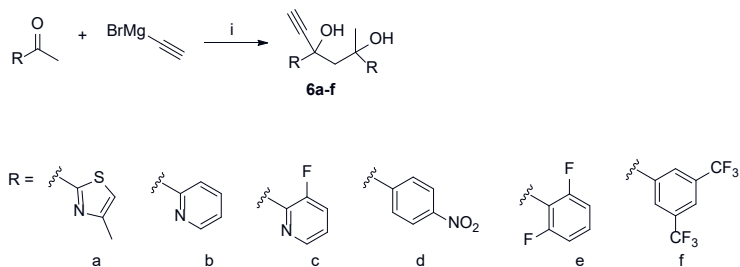


Scheme 1. Reagents and conditions: (i) NaH, THF, 0 °C; (ii) NaBH<sub>4</sub>·I<sub>2</sub>, THF, 0 °C; (iii) MsCl, Et<sub>3</sub>N, DCM, 0 °C; (iv) NaN<sub>3</sub>, DMF, 65 °C; (v) *n*-BuLi, THF, –80 °C; (vi) TBAF, r.t.; (vii) tris(triphenylphosphine) copper(I) bromide, DCM, 40 °C.

yields of **6** were obtained at 0 °C and when 2 equivalents of ethynylmagnesium bromide were used. Notably, the significant formation of 1,3-diols occurred only when the aryl methyl ketones featured aryl groups with electron-withdrawing properties. In contrast, aryl methyl ketones with electron-donating substituents (*e.g.*, 4-methoxyacetophenone) predominantly underwent direct addition of ethynylmagnesium bromide to the carbonyl group.

Regarding the reaction mechanism, we propose a tentative pathway (Scheme 3) to rationalise the formation of 1,3-diols. In the first step, ethynylmagnesium bromide likely acts as a base, deprotonating the methyl group of the aryl methyl ketone to generate an enolate anion. This enolate may then attack the carbonyl group of another aryl methyl ketone, resulting in the formation of a keto-alkoxide intermediate. The requirement for sufficient acidity in the starting aryl methyl ketones could explain why electron-withdrawing groups in the aryl moiety facilitate the reaction. Subsequently, a nucleophilic attack by ethynylmagnesium bromide on the carbonyl group of the intermediate may lead, after protonation, to the formation of the 1,3-diol product **6**.

The absolute stereochemistry of compounds **6c** and **6e** was determined by single-crystal X-ray diffraction and confirmed to be a mixture of the (*R,R*)- and (*S,S*)-enantiomers. Based

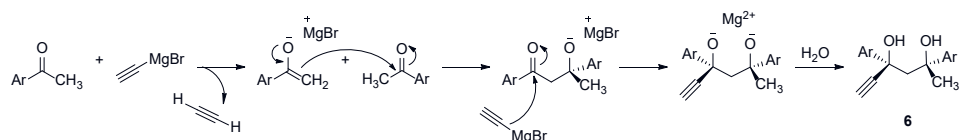


Scheme 2. Reagents and conditions: (i) THF, 0 °C.

on the  $^1\text{H}$  NMR spectra, compounds **6b**, **6d**, and **6f** are also presumed to be diastereomerically pure, likely representing the same pair of enantiomers. In contrast, the  $^1\text{H}$  and  $^{13}\text{C}$  NMR spectra of compound **6a** show duplicated signals, indicative of a mixture of diastereomers. While additional experiments specifically focused on elucidating the stereochemical course of the reaction would provide more definitive insights, such studies fall beyond the scope of the present work.

Similar 1,3-diol structures have been previously reported by Jiao and co-workers (46, 47), who utilised isopropenyl acetate as the starting material in reactions with either aryl or arylalkynyl Grignard reagents, yielding 1,3-diols predominantly in the *anti*-configuration. In contrast, although the present methodology was not primarily designed to control stereochemistry, it appears to preferentially afford 1,3-diols with the *syn*-configuration, as confirmed by X-ray crystallographic analysis of selected products (with the exception of compound **6a**). This divergence in stereochemical outcome underscores the complementary nature of our transformation and provides an alternative route to access stereochemically defined 1,3-diols.

Compound **6c** crystallises in the centrosymmetric group  $P2_1/c$  with two molecules in the asymmetric unit (Fig. 3). The fluoropyridyl rings are stacked at a  $17.12^\circ$  angle and centroid-centroid distance of  $3.578 \text{ \AA}$ . This conformation is further locked by two intramolecular hydrogen bonds  $\text{O13-H13}\cdots\text{O10}$  ( $d(\text{H-O}) = 2.051 \text{ \AA}$ ) and  $\text{O10-H10}\cdots\text{N1}$  ( $d(\text{H-N}) = 1.905 \text{ \AA}$ ). On the other hand, compound **6e** also crystallizes in a centrosymmetric group with two molecules, both the *S,S* and the *R,R* enantiomer in the asymmetric unit (Fig. 3). The difluorophenyl rings are in a stacked conformation as well, with smaller slanting with angles between aromatic ring planes of  $13.63^\circ$  and  $14.56^\circ$  and a shorter centroid-centroid distances ( $3.511 \text{ \AA}$  and  $3.470 \text{ \AA}$ ). The molecule B in the crystal structure shows a partial racemic disorder evidenced by residual electron density ( $2.27 \text{ eA}^{-3}$ ) in proximity of the methyl group and a slightly larger ellipsoid size of the terminal acetylene C atom, how-



Scheme 3. Proposed reaction mechanism for the formation of 1,3-diols.

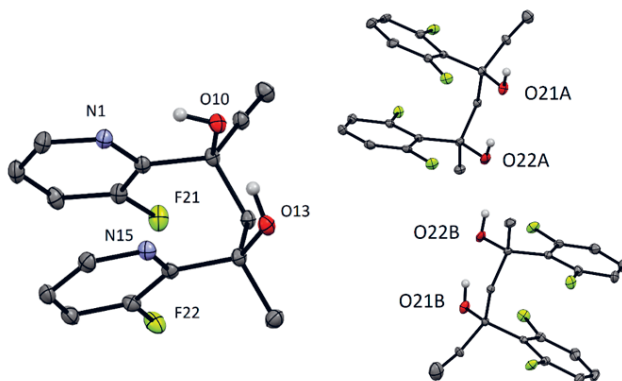


Fig. 3. Crystal structures of compounds **6c** (left) and **6e** (right). Thermal ellipsoids are drawn at 35 % probability level. Only hydrogen atoms bound to heteroatoms are shown for better clarity.

ever, we were unable to refine the structural model using positional disorder (Table III). The hydrogen bond network is different as molecules form a catemer along the crystallographic axis *a*. The bond distance values in the O21B–H21B...O22B, O22B–H22B...O22A, O22A–H22A...O21A, O21A–H21A...O21B' catemer range from 1.870 Å to 1.972 Å.

### Synthesis of tetrahydropyran-based compounds

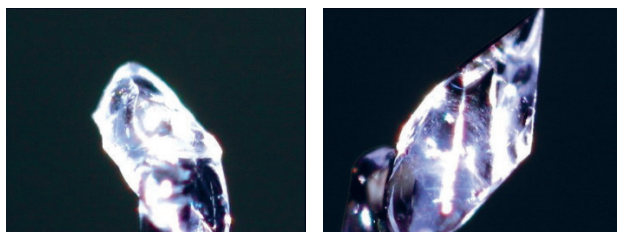
For the tetrahydropyran series, azide **7** was synthesised from 4-(azidomethyl)benzoic acid and (4-(4-phenylthiazol-2-yl)tetrahydro-2*H*-pyran-4-yl)methanamine (**21**) *via* the corresponding acid chloride intermediate. In the next step, a CuAAC reaction between azide **7** and various small alkynes was carried out to yield the final compounds, except for **8a** and **8e**, which required additional transformations (Scheme 4). For compound **8a**, trimethylsilylacetylene was used as the alkyne reagent, and the resulting product underwent treatment with TBAF to remove the trimethylsilyl moiety. Compound **8e** was obtained by hydrolysis of ethyl ester **8d**.

Table III. Crystal data and structure refinement for **6c** and **6e**

Compd.	<b>6c</b>	<b>6e</b>
Sample code	moc70	moc61
CCDC deposition number	2425328	2425329
Empirical formula	C <sub>16</sub> H <sub>14</sub> F <sub>2</sub> N <sub>2</sub> O <sub>2</sub>	C <sub>18</sub> H <sub>14</sub> F <sub>4</sub> O <sub>2</sub>
Relative molecular mass	304.29	338.29
Temperature/K	150.00(10)	150.00(10)
Crystal system	monoclinic	monoclinic
Space group	P2 <sub>1</sub> /c	P2 <sub>1</sub> /n
<i>a</i> /Å	8.0271 (3)	12.5027(6)
<i>b</i> /Å	16.8908(6)	16.3529(8)

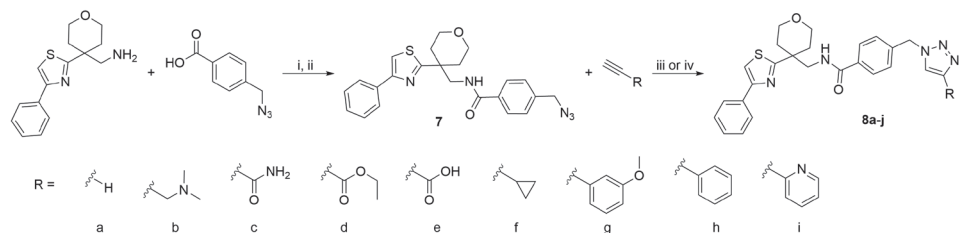
Compd.	6c	6e
$c/\text{\AA}$	10.8155(4)	14.7705(7)
$\alpha/^\circ$	90	90
$\beta/^\circ$	104.716(4)	93.449(5)
$\gamma/^\circ$	90	90
Volume/ $\text{\AA}^3$	1418.31(9)	3014.4 (3)
Z	4	8
$\rho_{\text{calc}} \text{ g cm}^{-3}$	1.425	1.491
$\mu/\text{mm}^{-1}$	0.113	0.129
F(000)	632.0	1392.0
Crystal size/ $\text{mm}^3$	$0.3 \times 0.3 \times 0.2$	$0.6 \times 0.4 \times 0.4$
Radiation	Mo K $\alpha$ ( $\lambda = 0.71073$ )	Mo K $\alpha$ ( $\lambda = 0.71073$ )
$2\Theta$ range for data collection/ $^\circ$	4.824 to 54.958	4.838 to 58.816
Index ranges	$-9 \leq h \leq 10$ , $-21 \leq k \leq 21$ , $-13 \leq l \leq 13$	$-17 \leq h \leq 15$ , $-17 \leq k \leq 22$ , $-15 \leq l \leq 20$
Reflections collected	18761 3225	13311 7077
Independent reflections	[ $R_{\text{int}} = 0.0322$ , $R_{\text{sigma}} = 0.0232$ ]	[ $R_{\text{int}} = 0.0251$ , $R_{\text{sigma}} = 0.0407$ ]
Data/restraints/parameters	3225/0/205	7077/0/439
Goodness-of-fit on $F^2$	1.055	1.085
Final R indexes [ $I > 2\sigma(I)$ ]	$R_1 = 0.0373$ , $wR_2 = 0.0851$	$R_1 = 0.0965$ , $wR_2 = 0.2632$
Final R indexes [all data]	$R_1 = 0.0499$ , $wR_2 = 0.0945$	$R_1 = 0.1211$ , $wR_2 = 0.2827$
Largest diff. peak/hole / $e \text{ \AA}^{-3}$	0.30/-0.22	2.27/-0.59

Photographs of the crystals



### *InhA inhibition testing results*

The prepared compounds were evaluated for their ability to inhibit InhA. Among the thiadiazole-based compounds, only compound **5a**, a direct analogue of the lead compound, exhibited activity, with an  $IC_{50}$  of  $11 \mu\text{mol L}^{-1}$ . All other compounds in this series



Scheme 4. Reagents and conditions: (i) oxalyl chloride,  $\text{DMF}_{\text{cat}}$ ,  $\text{CH}_2\text{Cl}_2$ ,  $0^\circ\text{C}$ ; (ii)  $\text{Et}_3\text{N}$ ,  $\text{CH}_2\text{Cl}_2$ , THF,  $0^\circ\text{C}$ ; (iii)  $\text{CuBr}$ ,  $\text{Et}_3\text{N}$ ,  $\text{EtOAc/MeOH}$ ,  $40^\circ\text{C}$ ; (iv) tris(triphenylphosphine)copper(I) bromide, DCM,  $40^\circ\text{C}$ .

were inactive. According to the crystal structure of the thiazazole lead compound, the nitrogen atom in the thiazole ring forms a crucial hydrogen bond with the phosphate group of  $\text{NAD}^+$  in the active site of InhA. We hypothesised that compounds with nitrogen atoms in the *ortho* position, such as **5b**, **5e**, **5f**, and **5g**, would retain some activity by forming a similar hydrogen bond. However, these compounds were also inactive.

A potential explanation could be the spatial constraints of the binding pocket, which may accommodate only a thiazole ring and not larger six-membered heterocycles. Nevertheless, this does not account for the 1000-fold lower potency of **5a** compared to the lead compound ( $IC_{50} = 3 \text{ nmol L}^{-1}$ ) (17). The likely reason for this reduced activity is the loss of the hydrogen bond with Met198, which was also confirmed in our docking experiments (Fig. 4). The synthesis of the **5** series required replacing the amine group that connects the thiazazole and pyrrole moieties in the lead compound with a methylene group, leading to the loss of this key hydrogen bond.

InhA inhibition was also assessed using tetrahydropyran-based compounds **8a-j**. Among these, **8a**, the compound most structurally similar to the lead compound, showed the highest potency, with an  $IC_{50}$  of  $64 \mu\text{mol L}^{-1}$ . However, this represents a 1000-fold decrease in potency compared to the lead tetrahydropyran compound ( $IC_{50} = 20 \text{ nmol L}^{-1}$ ) (21). Additionally, **8d**, **8g**, and **8f** were poorly soluble and could not be fully tested; they showed no activity at lower concentrations. The loss of activity in this series is challenging to rationalize as even docking experiment could not explain it (Fig. 4). Based on the crystal structure, the nitrogen at position 2 of the pyrazole ring in the lead compound forms a hydrogen bond with the phosphate group of  $\text{NAD}^+$ , and the triazole in these analogues should be capable of a similar interaction. These results suggest that the structure-activity relationship of tetrahydropyran-based compounds is highly constrained and sensitive to modifications.

Testing the bactericidal activity of these compounds was deemed unnecessary due to their poor inhibitory performance. Nonetheless, the CuAAC click chemistry approach used in this study proved effective for rapidly generating a small library of compounds to explore the chemical space of the target active site. However, it is crucial that we ensure functional groups critical for key interactions with the target remain intact during compound modification. Furthermore, CuAAC introduces triazole heterocycles into the compounds, which may exacerbate solubility issues, especially if solubility was already a challenge with the lead compound.

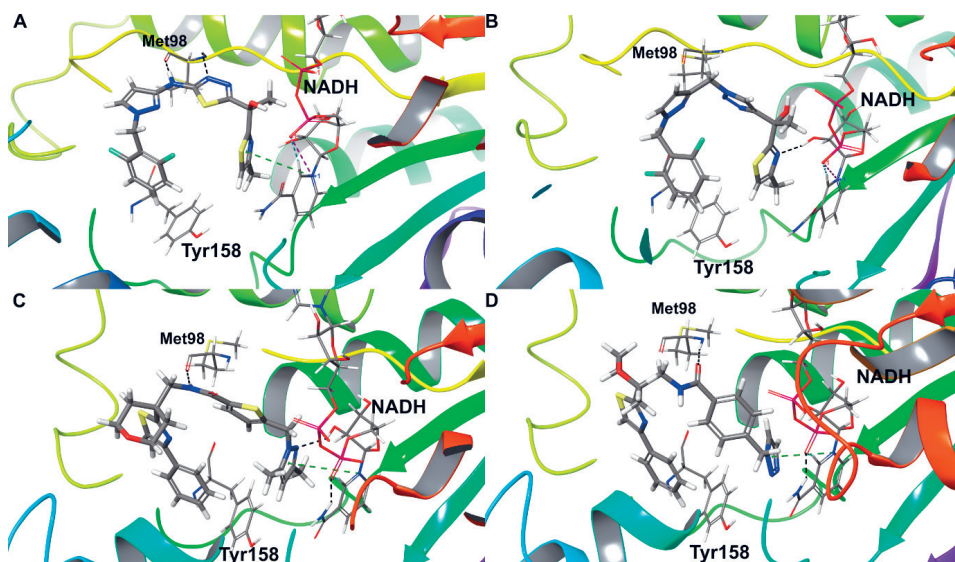


Fig. 4. Binding poses of thiadiazole (A) and tetrahydropyran (C) lead compounds into InhA binding site and a comparison with docked ligands 5a (B) and 8a (D).

## CONCLUSIONS

This study highlights the challenges of designing effective inhibitors for the InhA enzyme, even when starting with promising lead structures. Two series of inhibitors inspired by thiaziazole and tetrahydropyran lead compounds were synthesised using CuAAC click chemistry. This approach enabled the rapid and efficient generation of two small compound libraries. However, except for compound 5a, the synthesised inhibitors failed to demonstrate significant activity against InhA. For the thiadiazole-based compounds, the lack of activity was attributed to the substitution of the amine group with a methylene moiety. While the amine group forms a crucial hydrogen bond with Met98 in the active site, the methylene group lacks this capability. Similarly, the tetrahydropyran-based compounds were largely inactive, with poor solubility further compounding the issue. The inactivity of this series was likely due to the narrow SAR inherent to compounds with this scaffold. Despite the limited biological activity of the synthesised compounds, the study unveiled a novel reaction involving aryl methyl ketones and ethynylmagnesium bromide, producing 1,3-diols. The structure of these products was confirmed by X-ray crystallography, offering valuable contributions to the field of synthetic chemistry. These findings underscore the importance of preserving key structural features during inhibitor optimisation and highlight the utility of click chemistry for efficiently exploring chemical space. Future efforts should prioritise the retention of critical target interactions and the exploration of alternative scaffolds to develop more potent and selective InhA inhibitors.

*Conflicts of interest.* – The authors declare no conflict of interest.

*Funding.* – This work was supported by the Slovenian Research and Innovation Agency (ARIS; core research funding P1-0208 and P1-0175 and project grant J3-3079). The authors also acknowledge

the support of the Centre for Research Infrastructure at the University of Ljubljana, Faculty of Chemistry and Chemical Technology, which is part of the Network of Research and Infrastructural Centres UL (MRIC UL) and is financially supported by the Slovenian Research and Innovation Agency (ARIS; Infrastructure programme No. I0-0022) for the use of the Supernova diffractometer. M.J. acknowledges support by the research project 2200/04/2024-2026 as part of the “Competition for 2024-2026 Postdoctoral Job Positions at the University of Hradec Králové” at the Faculty of Science, University of Hradec Králové.

*Authors contributions.* – Conceptualisation, M.H.R. and S.P.; methodology, M.H.R., R.F., and I.S.; analysis, M.H.R. and R.F.; investigation, M.H.R., N.G., R.F., A.B., J.K., M.J., and S.P.; writing, original draft preparation, M.H.R., R.F., J.K., and S.P.; writing, review and editing, N.G., A.B., M.J., I.S., S.G., and S.P. All authors have read and agreed to the published version of the manuscript.

## REFERENCES

1. [https://www.who.int/health-topics/tuberculosis#tab=tab\\_1](https://www.who.int/health-topics/tuberculosis#tab=tab_1); last access date May 19, 2025.
2. Y. M. Jacobo-Delgado, A. Rodríguez-Carlos, C. J. Serrano and B. Rivas-Santiago, *Mycobacterium tuberculosis* cell-wall and antimicrobial peptides: a mission impossible?, *Front. Immunol.* **14** (2023) Article ID 1194923 (18 pages); <https://doi.org/10.3389/fimmu.2023.1194923>
3. S. S. R. Alsayed and H. Gunosewoyo, Tuberculosis: Pathogenesis, current treatment regimens and new drug targets, *IJMS* **24**(6) (2023) Article ID 5202 (23 pages); <https://doi.org/10.3390/ijms24065202>
4. M. S. Prasad, R. P. Bhole, P. B. Khedekar and R. V. Chikhale, Mycobacterium enoyl acyl carrier protein reductase (InhA): A key target for antitubercular drug discovery, *Bioorg. Chem.* **115** (2021) Article ID 105242; <https://doi.org/10.1016/j.bioorg.2021.105242>
5. S. Lale Ngema, N. Dookie, R. Perumal, L. Nandlal, N. Naicker, M. Peter Letsoalo, M. O'Donnell, A. Khan, N. Padayatchi and K. Naidoo, Isoniazid resistance-conferring mutations are associated with highly variable phenotypic resistance, *J. Clin. Tuberculosis Other Mycobacterial Dis.* **33** (2023) Article ID 100387 (6 pages); <https://doi.org/10.1016/j.jctube.2023.100387>
6. S. K. Wahan, G. Bhargava, V. Chawla and P. A. Chawla, Unlocking InhA: Novel approaches to inhibit *Mycobacterium tuberculosis*, *Bioorg. Chem.* **146** (2024) Article ID 107250; <https://doi.org/10.1016/j.bioorg.2024.107250>
7. S. L. Parikh, G. Xiao and P. J. Tonge, Inhibition of InhA, the enoyl reductase from *Mycobacterium tuberculosis*, by triclosan and isoniazid, *Biochemistry* **39**(26) (2000) 7645–7650; <https://doi.org/10.1021/bi0008940>
8. M. R. Kuo, H. R. Morbidoni, D. Alland, S. F. Sneddon, B. B. Gourlie, M. M. Staveski, M. Leonard, J. S. Gregory, A. D. Janjigian, C. Yee, J. M. Musser, B. Kreiswirth, H. Iwamoto, R. Perozzo, W. R. Jacobs, J. C. Sacchettini and D. A. Fidock, Targeting tuberculosis and malaria through inhibition of enoyl reductase, *J. Biol. Chem.* **278**(23) (2003) 20851–20859; <https://doi.org/10.1074/jbc.M211968200>
9. T. S. Ibrahim, E. S. Taher, E. Samir, A. M. Malebari, A. N. Khayyat, M. F. A. Mohamed, R. M. Bokhtia, M. A. AlAwadh, I. A. Seliem, H. Z. Asfour, N. A. Alhakamy, S. S. Panda and A. M. M. AL-Mahmoudy, In vitro antimycobacterial activity and physicochemical characterization of diaryl ether triclosan analogues as potential InhA reductase inhibitors, *Molecules* **25**(14) (2020) Article ID 3125 (18 pages); <https://doi.org/10.3390/molecules25143125>
10. T. Armstrong, M. Lamont, A. Lanne, L. J. Alderwick and N. R. Thomas, Inhibition of *Mycobacterium tuberculosis* InhA: Design, synthesis and evaluation of new di-triclosan derivatives, *Bioorg. Med. Chem.* **28** (2020) Article ID 115744; <https://doi.org/10.1016/j.bmc.2020.115744>
11. F. Rodriguez, N. Saffon, J. C. Sammartino, G. Degiacomi, M. R. Pasca and C. Lherbet, First triclosan-based macrocyclic inhibitors of InhA enzyme, *Bioorg. Chem.* **95** (2020) Article ID 103498; <https://doi.org/10.1016/j.bioorg.2019.103498>

12. X. He, A. Alian and P. R. Ortiz De Montellano, Inhibition of the *Mycobacterium tuberculosis* enoyl acyl carrier protein reductase InhA by arylamides, *Bioorg. Med. Chem.* **15** (2007) 6649–6658; <https://doi.org/10.1016/j.bmc.2007.08.013>
13. A. Chollet, G. Mori, C. Menendez, F. Rodriguez, I. Fabing, M. R. Pasca, J. Madacki, J. Korduláková, P. Constant, A. Quémar, V. Bernardes-Génisson, C. Lherbet and M. Baltas, Design, synthesis and evaluation of new GEQ derivatives as inhibitors of InhA enzyme and *Mycobacterium tuberculosis* growth, *Eur. J. Med. Chem.* **101** (2015) 218–235; <https://doi.org/10.1016/j.ejmech.2015.06.035>
14. U. H. Manjunatha, S. P. S. Rao, R. R. Kondreddi, C. G. Noble, L. R. Camacho, B. H. Tan, S. H. Ng, P. S. Ng, N. L. Ma, S. B. Lakshminarayana, M. Herve, S. W. Barnes, W. Yu, K. Kuhen, F. Blasco, D. Beer, J. R. Walker, P. J. Tonge, R. Glynn, P. W. Smith and T. T. Diagana, Direct inhibitors of InhA are active against *Mycobacterium tuberculosis*, *Sci. Transl. Med.* **7**(269) (2015) Article ID p.269ra3; <https://doi.org/10.1126/scitranslmed.3010597>
15. F. Roquet-Banères, M. Alcaraz, C. Hamela, J. Abendroth, T. E. Edwards and L. Kremer, *In vitro* and *in vivo* efficacy of NITD-916 against *Mycobacterium fortuitum*, *Antimicrob. Agents Chemother.* **67**(4) (2023) e01607-22; <https://doi.org/10.1128/aac.01607-22>
16. Y. Xia, Y. Zhou, D. S. Carter, M. B. McNeil, W. Choi, J. Halladay, P. W. Berry, W. Mao, V. Hernandez, T. O'Malley, A. Korkegian, B. Sunde, L. Flint, L. K. Woolhiser, M. S. Scherman, V. Gruppo, C. Hastings, G. T. Robertson, T. R. Ioerger, J. Sacchettini, P. J. Tonge, A. J. Lenaerts, T. Parish and M. R. K. Alley, Discovery of a cofactor-independent inhibitor of *Mycobacterium tuberculosis* InhA, *Life Sci. Alliance* **1**(3) (2018) e201800025; <https://doi.org/10.26508/lsa.201800025>
17. P. S. Shirude, P. Madhavapeddi, M. Naik, K. Murugan, V. Shinde, R. Nandishaiah, J. Bhat, A. Kumar, S. Hameed, G. Holdgate, G. Davies, H. McMiken, N. Hegde, A. Ambady, J. Venkatraman, M. Panda, B. Bandodkar, V. K. Sambandamurthy and J. A. Read, Methyl-thiazoles: A novel mode of inhibition with the potential to develop novel inhibitors targeting InhA in *Mycobacterium tuberculosis*, *J. Med. Chem.* **56** (21) (2013) 8533–8542; <https://doi.org/10.1021/jm4012033>
18. M. Martínez-Hoyos, E. Perez-Herran, G. Gulten, L. Encinas, D. Álvarez-Gómez, E. Alvarez, S. Ferrer-Bazaga, A. García-Pérez, F. Ortega, I. Angulo-Barturen, J. Rullas-Trincado, D. Blanco Ruano, P. Torres, P. Castañeda, S. Huss, R. Fernández Menéndez, S. González Del Valle, L. Ballell, D. Barros, S. Modha, N. Dhar, F. Signorin-Gelo, J. D. McKinney, J. F. Garcia-Bustos, J. L. Lavandera, J. C. Sacchettini, M. Soledad Jimenez, N. Martin-Casabona, J. Castro-Pichel and A. Mendoza-Losana, Antitubercular drugs for an old target: GSK693 as a promising InhA direct inhibitor, *eBioMed.* **8** (2016) 291–301; <https://doi.org/10.1016/j.ebiom.2016.05.006>
19. R. Šink, I. Sosič, M. Živec, R. Fernandez-Menendez, S. Turk, S. Pajk, D. Alvarez-Gomez, E. M. Lopez-Roman, C. Gonzales-Cortez, J. Rullas-Triconado, I. Angulo-Barturen, D. Barros, L. Ballell-Pages, R. J. Young, L. Encinas and S. Gobec, Design, synthesis, and evaluation of new thiadiazole-based direct inhibitors of enoyl acyl carrier protein reductase (InhA) for the treatment of tuberculosis, *J. Med. Chem.* **58**(2) (2015) 613–624; <https://doi.org/10.1021/jm501029r>
20. L. Encinas, S.-Y. Li, J. Rullas-Trincado, R. Tasneen, S. Tyagi, H. Soni, A. Garcia-Perez, J. Lee, R. González Del Río, J. De Mercado, V. Sousa, I. Sosič, S. Gobec, A. Mendoza-Losana, P. J. Converse, K. Mdluli, N. Fotouhi, D. Barros-Aguirre and E. L. Nuermberger, Contribution of direct InhA inhibitors to novel drug regimens in a mouse model of tuberculosis, *Antimicrob. Agents Chemother.* **68**(11) (2024) e00357-24; <https://doi.org/10.1128/aac.00357-24>
21. S. Pajk, M. Živec, R. Šink, I. Sosič, M. Neu, C. Chung, M. Martínez-Hoyos, E. Pérez-Herrán, D. Álvarez-Gómez, E. Álvarez-Ruiz, A. Mendoza-Losana, J. Castro-Pichel, D. Barros, L. Ballell-Pages, R. J. Young, M. A. Convery, L. Encinas and S. Gobec, New direct inhibitors of InhA with antimycobacterial activity based on a tetrahydropyran scaffold, *Eur. J. Med. Chem.* **112** (2016) 252–257; <https://doi.org/10.1016/j.ejmech.2016.02.008>
22. J. S. Freundlich, F. Wang, C. Vilchèze, G. Gulten, R. Langley, G. A. Schiehser, D. P. Jacobus, W. R. Jacobs and J. C. Sacchettini, Triclosan derivatives: Towards potent inhibitors of drug-sensitive and drug-resistant *Mycobacterium tuberculosis*, *ChemMedChem* **4**(2) (2009) 241–248; <https://doi.org/10.1002/cmdc.200800261>

23. J. K. Barbay, W. Chai, W. Eccles, M. D. Hack, A. T. Herrmann, W. M. Jones, P. J. Krawczuk, K. D. Kreutter, A. D. Lebsack, D. J. Pippel, A. R. Rovira and R. L. Wolin, *Small Molecule Inhibitors of NF- $\kappa$ B Inducing Kinase*, WO 2020/239999 A1, 3 Dec 2020.
24. J. Song, Y. Zhu, W. Zu, C. Duan, J. Xu, F. Jiang, X. Wang, S. Li, C. Liu, Q. Gao, H. Li, Y. Zhang, W. Tang, T. Lu and Y. Chen, The discovery of quinoline derivatives, as NF- $\kappa$ B inducing kinase (NIK) inhibitors with anti-inflammatory effects in vitro, low toxicities against T cell growth, *Bioorg. Med. Chem.* **29** (2021) Article ID 115856; <https://doi.org/10.1016/j.bmc.2020.115856>
25. M. Isomura, D. A. Petrone and E. M. Carreira, Coordination-induced stereocontrol over carbocations: Asymmetric reductive deoxygenation of racemic tertiary alcohols, *J. Am. Chem. Soc.* **141**(11) (2019) 4738–4748; <https://doi.org/10.1021/jacs.9b00862>
26. M. R. Hall, M. Korb, S. A. Moggach and P. J. Low, Oxidative coupling of ruthenium alkenyl acetylide complexes as a route to dinuclear complexes featuring carbon-rich bridging ligands, *Organometallics* **41**(21) (2022) 2958–2973; <https://doi.org/10.1021/acs.organomet.2c00402>
27. G. Castanedo, J. Feng, C. A. G. N. Montalbetti, S. Staben, *Tricyclic Compounds and Methods of Use Therefor*, WO 2013/120980 A1, 22 Aug 2013.
28. S. M. Min, F. M. Bashore, J. L. Smith, T. M. Havener, S. Howell, H. Li, R. M. Couñago, K. I. Popov and A. D. Axtman, Development of a second-generation, *in vivo* chemical probe for PIKfyve, *J. Med. Chem.* **68**(3) (2025) 3282–3308; <https://doi.org/10.1021/acs.jmedchem.4c02531>
29. L.-H. Chung, C.-F. Yeung, D.-L. Ma, C.-H. Leung and C.-Y. Wong, Metal-indolizine zwitterion complexes as a new class of organometallic material: A spectroscopic and theoretical investigation, *Organometallics* **33**(13) (2014) 3443–3452; <https://doi.org/10.1021/om5003705>
30. X. Wang, Q. Chen, J. Zhou, Y. Hu, S. Ye and J. Wu, Electrochemical synthesis of alkenylsulfonates from alkynes, NaHSO<sub>3</sub> and alcohols, *Chin. J. Chem.* **43**(3) (2025) 292–296; <https://doi.org/10.1002/cjoc.202400962>
31. T. Zha, J. Rui, Z. Zhang, D. Zhang, Z. Yang, P. Yu, Y. Wang, F. Peng and Z. Shao, Direct catalytic asymmetric and regiodivergent N1- and C3-allylic alkylation of indoles, *Angew. Chem. Int. Ed.* **62**(21) (2023) Article ID e202300844; <https://doi.org/10.1002/anie.202300844>
32. G. S. Sontakke, A. K. Chaturvedi, D. Jana and C. M. R. Volla, Pyrazolidinone-aided Ru(II)-catalyzed regioselective C–H annulation with allenes, *Org. Lett.* **26**(21) (2024) 4480–4485; <https://doi.org/10.1021/acs.orglett.4c01245>
33. L.-B. Han, Y. Ono and H. Yazawa, Nickel-catalyzed addition of P(O)–H bonds to propargyl alcohols: One-pot generation of phosphinoyl 1,3-butadienes, *Org. Lett.* **7**(14) (2005) 2909–2911; <https://doi.org/10.1021/ol0508431>
34. M. R. Hall, S. A. Moggach and P. J. Low, Syntheses and structures of *trans*-bis(alkenylacetylide) ruthenium complexes, *Chemistry An Asian Journal* **16**(21) (2021) 3385–3403; <https://doi.org/10.1002/asia.202100850>
35. Y.-T. Gu, D.-D. Chen, C.-B. Wang, Q. Cheng, J.-R. Han, X. Tian, S. Liu and W. Su, A mild and general *trans*-diboration of both terminal and internal propargyl alcohols, *Org. Lett.* **26**(49) (2024) 10499–10504; <https://doi.org/10.1021/acs.orglett.4c03841>
36. Q. Tao, H. Zhang, R. Ye, Y. Zhang, Y. Long and X. Zhou, Palladium-catalyzed synthesis of  $\beta$ -alkynyl ketones via selective 1,3-alkynyl migration of  $\alpha,\alpha$ -disubstituted allylic alcohols, *J. Org. Chem.* **89**(18) (2024) 13208–13214; <https://doi.org/10.1021/acs.joc.4c01332>
37. P. A. Baghurst and L. W. Nichol, The binding of organic phosphates to human methaemoglobin A. Perturbation of the polymerization of proteins by effectors, *Biochim. Biophys. Acta* **412**(1) (1975) 168–180; [https://doi.org/10.1016/0005-2795\(75\)90349-9](https://doi.org/10.1016/0005-2795(75)90349-9)
38. O. V. Dolomanov, L. J. Bourhis, R. J. Gildea, J. A. K. Howard and H. Puschmann, OLEX2: a complete structure solution, refinement and analysis program, *J. Appl. Crystallography* **42** (2009) 339–341; <https://doi.org/10.1107/S0021889808042726>

39. A. Giuliani, The application of principal component analysis to drug discovery and biomedical data, *Drug Discov. Today* **22**(7) (2017) 1069–1076; <https://doi.org/10.1016/j.drudis.2017.01.005>
40. C. F. Macrae, P. R. Edgington, P. McCabe, E. Pidcock, G. P. Shields, R. Taylor, M. Towler and J. van de Streek, Mercury: visualization and analysis of crystal structures, *J. Appl. Crystallography* **39** (2006) 453–457; <https://doi.org/10.1107/S002188980600731X>
41. Schrödinger Release 2023-1: Maestro, Schrödinger, LLC, New York 2021.
42. N. M. O'Boyle, M. Banck, C. A. James, C. Morley, T. Vandermeersch and G. R. Hutchison, Open Babel: An open chemical toolbox, *J. Cheminformatics* **3** (2011) Article ID 33 (14 pages); <https://doi.org/10.1186/1758-2946-3-33>
43. R. A. Friesner, J. L. Banks, R. B. Murphy, T. A. Halgren, J. J. Klicic, D. T. Mainz, M. P. Repasky, E. H. Knoll, M. Shelley, J. K. Perry, D. E. Shaw, P. Francis and P. S. Shenkin, Glide: A new approach for rapid, accurate docking and scoring. 1. Method and assessment of docking accuracy, *J. Med. Chem.* **47**(7) (2004) 1739–1749; <https://doi.org/10.1021/jm0306430>
44. Schrödinger Release 2023-1: LigPrep, Schrödinger, LLC, New York 2021.
45. J. C. Shelley, A. Cholleti, L. L. Frye, J. R. Greenwood, M. R. Timlin and M. Uchimaya, Epik: A software program for pK(a) prediction and protonation state generation for drug-like molecules, *J. Comput. Aided Mol. Des.* **21** (2007) 681–691; <https://doi.org/10.1007/s10822-007-9133-z>
46. Y. Jiao, C. Cao and Z. Zhou, Direct synthesis of *anti*-1,3-diols through nonclassical reaction of aryl Grignard reagents with isopropenyl acetate, *Org. Lett.* **13**(2) (2011) 180–183; <https://doi.org/10.1021/ol102520y>
47. Y. Jiao, W. Zhao, S. Deng, Z. Tang, W. Liu, Y. Wan and F. Zhong, A one-pot diastereoselective synthesis of 1,3-diols and 1,3,5-triols via cascade reactions of arylalkynyl Grignard reagents with enol esters, *J. Chem. Res.* **44**(5-6) (2020) 255–266; <https://doi.org/10.1177/1747519820908513>